Photoreceptor Telodendria Morphology and Connectivity in the Zebrafish Retina

by

Nicole C. L. Noel

A thesis submitted in partial fulfillment of the requirements for the degree of

Master of Science

in

Physiology, Cell, and Developmental Biology

Department of Biological Sciences
University of Alberta

ABSTRACT

Photoreceptors (the light-sensitive cellular mediators of vision in the eye) are divided into two classes: rods, which are sensitive to dim light and responsible for vision in low-light conditions, and cones, which are sensitive to specific wavelengths of light, and are responsible for daytime and colour vision. Photoreceptors must relay information to other retinal neurons for light information to be modified and sent to the brain for interpretation. If photoreceptors are not connecting to, and communicating with, the appropriate cells, transmission of light information fails, and no image will be produced. Therefore, the connectivity amongst photoreceptors is critical to their function, as it underpins lateral inhibition and effective translation of stimuli into neural signals. Despite much work characterizing second-order interneurons in the outer retina, the synapses directly connecting photoreceptors have often been overlooked. Telodendria are fine processes that connect photoreceptor pedicles. They have been observed in diverse vertebrate groups, yet their roles in vision remain speculative. Here, I visualized and characterized telodendria via fluorescent protein expression in photoreceptor subtypes.

I characterized short wavelength cone telodendria in adult and larval zebrafish retina. Additionally, in the larval retina, I investigated rod telodendria and UV cone telodendria in mutant and transgenic retinas with altered complements of cone types. In the adult retina, telodendria are twice as abundant and branch almost twice as often on blue cones compared to UV cones. Pedicles of neighbouring UV and blue cones typically converge into contiguous pairs, despite the regular spacing of their cell bodies. In contrast to adults, larval UV cone telodendria are more numerous (1.3 times) than blue cone telodendria. UV cone telodendria are not detectably affected by ablation of blue cones, and are reduced 2-fold in mutant larval retina with few UV cones. I thus saw no evidence that telodendria increase in number in the absence of their typical cellular neighbours. I also found that larval rod telodendria are less

abundant than short wavelength cone telodendria. In summary, I describe the development and morphology of zebrafish photoreceptor synaptic connectivity towards appreciating the function of telodendria in visual signal processing.

PREFACE

This thesis is an original work by Nicole C. L. Noel.

Approval for this study was obtained from the Animal Care and Use Committee: BioSciences, under protocol AUP00000077.

Figure 2 is modified from a figure designed for an assignment for a graduate course (MDGEN 605). W. Ted Allison provided confocal images of sectioned zebrafish retina for Figure 5, Figure 6A,B, and Figure 7B.

Chapter 2 is modified from a manuscript submission that was accepted in *Journal of Comparative Neurology*, N. C. L. Noel and W. T. Allison, "Connectivity of Cone Photoreceptor Telodendria in the Zebrafish Retina." This thesis abstract is modified from the manuscript abstract in N. C. L. Noel and W. T. Allison, "Connectivity of Cone Photoreceptor Telodendria in the Zebrafish Retina."

ACKNOWLEDGEMENTS

I would like to thank my supervisor, Dr. Ted Allison, for giving me the opportunity to join the Allison lab as an undergraduate and giving me my first exposure to research. I appreciate all of Ted's support, guidance, and mentorship throughout my graduate program. I would also like to thank my wonderful committee members, Dr. Ian MacDonald and Dr. Heather McDermid, for their invaluable support and feedback.

I would like to thank all the members of the Allison lab, past and present, for always being so pleasant and making the working environment enjoyable. Thank you to Phil Oel for encouraging me to try research when I was an undergrad, and for all of his mentorship since – I don't know if I would have ended up where I am, otherwise.

Throughout my undergraduate and graduate career, I have been lucky to meet and learn from many excellent professors, lab coordinators, and TAs, all of whom I am grateful for. Many thanks to Dr. Dave Pilgrim for his encouragement and support. Thank you to Dr. Kendal Prill for all her help throughout my undergrad, grad school, and thesis writing – I am extremely grateful.

Thank you to the Department of Biological Sciences for providing me with a Teaching Assistantship, as well as the Faculty of Graduate Studies and Research.

Finally, thank you to my family for their unwavering support throughout my academic career. Thank you to my parents for always being patient and supportive, no matter what endeavours I embarked on. Thanks to my brother and sister, Mitchell and Lacey, for always lifting my spirits.

TABLE OF CONTENTS

LIST OF TABLES

LIST OF FIGURES

LIST OF ABBREVIATIONS

AAV	adeno-associated virus
AMD	age related macular degeneration
Cas	CRISPR associated protein
CMZ	ciliary marginal zone
CRISPR	clustered regularly interspaced short palindromic repeat
Dpf	days post fertilization
DMSO	dimethyl sulfoxide
EIAV	equine infectious anemia virus
ESC	embryonic stem cell
GCL	ganglion cell layer
GFP	green fluorescent protein
gRNA	guide RNA
HC	horizontal cell
Hpf	hours post fertilization
INL	inner nuclear layer
IPL	inner plexiform layer
IS	inner segment
iPSC	induced pluripotent stem cell
MS-222	tricaine methanesulfonate
MTZ	metronidazole
NTR	nitroreductase
NRL	neural retina-specific leucine zipper
OMR	optomotor response
ONL	outer nuclear layer

OPL	outer plexiform layer
OS	outer segment
PTU	1-phenol-2-thiourea
RdCVF	rod-derived cone viability factor, short chain
RdCVFL	rod-derived cone viability factor, long chain
RGC	retinal ganglion cell
RP	retinitis pigmentosa
RPE	retinal pigmented epithelium
UV	ultraviolet

1 INTRODUCTION

1.1 Retinal organization

Vision requires communication between a complex network of cells within the retina. Broadly, this network consists of five classes of retinal neurons: photoreceptors, bipolar cells, horizontal cells, amacrine cells, and retinal ganglion cells. There are two distinct types of retinal photoreceptors responsible for facilitating vision: cone photoreceptors, which are maximally sensitive to specific wavelengths of light, and allow for daytime/color vision; and rod photoreceptor cells, which are extremely sensitive and can detect single photons, allowing for vision under dim light conditions. The retinal layer that the photoreceptor cells are situated in is referred to as the outer nuclear layer (ONL). The photoreceptors have an outer segment (OS), which, in the case of rods, contain membranous discs densely studded with the photosensitive rhodopsin protein. These membranous discs are encapsulated by another membrane. In the case of cones, the OS is comprised of stacked lamellae that contain opsin proteins, which are sensitive to particular wavelengths of light, and are not surrounded by an additional membrane – rather, the lamellae are exposed to the extracellular matrix. These OSs are in contact with the retinal pigment epithelium (RPE), which provides nutrients and collects pieces of OSs that have been shed by the photoreceptor cells. Next is the photoreceptor inner segment (IS), a specialized mitochondria-rich compartment, followed by the nucleus, and finally the synaptic body (referred to as the rod spherule, or cone pedicle), where the photoreceptors synapse with downstream neurons.

In order to mediate vision, photoreceptors must properly integrate into the rest of the developing neural retina, and form appropriate connections with downstream cells. In a functioning, developed retina, light information is vertically relayed from the

photoreceptor cells, to the bipolar cells, and then transmitted to the retinal ganglion cells (RGCs) (Figure 1). Horizontal cells provide lateral inhibition and modification of input from photoreceptors to the bipolar cells. The location of synapses between the photoreceptors, bipolar, and horizontal cells is the outer plexiform layer (OPL). Amacrine cells influence the output of bipolar cells by lateral inhibition. The horizontal, bipolar, and amacrine cells comprise the inner nuclear layer (INL). The location of amacrine and ganglion cell contacts is the inner plexiform layer (IPL). RGCs transmit visual information from the retina to the brain, and the ganglion cell axons form the optic nerve. The RGCs sit in the ganglion cell layer (GCL).

Perturbations in this complex neural network can lead to inefficient or inappropriate relaying of information, which ultimately results in visual impairment. Understanding how photoreceptors form connections with other cells, and the nature of these connections, is key for success of therapies that intend to deploy photoreceptor precursor cells to replace lost photoreceptor cells; if these differentiated photoreceptors cannot form proper connections, then recovery of vision will not be successful. This not only includes connections between photoreceptor cells and downstream bipolar and horizontal cells, but also encompasses cone-cone and cone-rod connections.

1.2 Inherited photoreceptor degenerations are irreparable causes of vision loss

Photoreceptors are the cellular mediators of vision, and their loss results in visual impairment. In humans, this loss is irreversible, as retinal neurons are not replaced in the mature retina. Photoreceptor degenerative diseases are categorized by the photoreceptor type that is initially afflicted, and can be grouped into rod and cone dystrophies. The

following are examples of the most common rod and cone degenerations, though there are many more than are mentioned here.

1.2.1 Rod dystrophies

1.2.1.1 Retinitis pigmentosa

Retinitis pigmentosa (RP; OMIM #268000) is a progressive rod degeneration characterized by night blindness, loss of peripheral vision, and eventual central vision loss. Alterations to the retinal pigmented epithelium result in "bone spicule" pigment deposits characteristic of RP. RP is the most common inherited photoreceptor degeneration, affecting 1/3500 to 1/5000 individuals. RP is extremely heterogeneous, with more than 60 genes linked to non-syndromic forms of RP, and can be inherited in an autosomal recessive, dominant, X-linked, digenic, or mitochondrial manner [1-4].

The genetic heterogeneity of RP poses challenges in developing gene-based treatments. Therapies to treat the specific genetic lesion are appealing, but would rely on identifying the causative mutation on a patient-by-patient basis and tailoring the strategy accordingly, which can be difficult. Mutations in *rhodopsin* (*RHO*) are the most frequent causes of autosomal dominant RP, but loss-of-function mutations in *RHO* can also result in autosomal recessive RP [5-8]. Over 100 mutations in *RHO* have been linked to autosomal dominant RP, demonstrating how complex developing treatment strategies that target specific genetic lesions would be [9].

In RP, rods degenerate while cones persist; however, cones eventually degenerate as well. The reason for cone degeneration after rod loss is unknown, especially since the genetic lesions that lead to RP are typically rod-specific genes, such as *RHO*. Understanding why cones degenerate following rod death could allow for prevention of

the subsequent cone photoreceptors death, allowing for preservation of central vision in patients with advanced RP.

One possibility is that rods secrete trophic factors necessary for cone survival. Indeed, it was found that factors secreted from rods contribute to cone survival, and a trophic factor called rod-derived cone viability factor was identified [10, 11]. Two isoforms of rod-derived cone viability factor exist, a truncated form (RdCVF) and a long-chain form (RdCVFL). In rodent models of RP, RdCVF expression was found to increase cone survival, while RdCVFL prolonged rod functionality [10, 12, 13].

There is also support for cone nutrient deficiency after rod degeneration. For example, the mechanistic target of rapamycin (mTOR) pathway is involved in cellular metabolism and was down regulated in the retina of RP animal model [14, 15]. Glucose-inducible genes were also down regulated in cones after rod loss, suggesting that cones were glucose deprived [16]. Wang *et al.* found that, in a swine model of RP, glucose was sequestered to the RPE and not found in cones post rod death [16]. The cones could be reactivated from their dormant (lacking ISs or OSs) state by either introducing wild-type rods to the retina or by subretinal injection of glucose, further supporting that the remaining cones were nutrient starved after rods degenerate.

Another possibility is that oxidative stress causes cone degeneration. In the human retina, rods account for the majority of the photoreceptor population, meaning that rods are the primary cells consuming oxygen delivered to the retina. After rod loss, oxygen levels increase within the retina, and reactive oxygen species can accumulate and cause damage to the cone cells as a result [17]. Antioxidant treatments can slow (though do not halt) progression of cone degeneration in animal models of RP, supporting the theory of oxidative stress harming cones after rod loss [18, 19].

Finally, the gap junction-mediated bystander effect could be leading to cone degeneration in RP. The gap junction-mediated bystander effect is a poorly investigated potential cause of cone degeneration in RP [20]. The mechanism responsible for this would involve toxins or pro-apoptotic signals being transmitted from dying cells to healthy cells via the photoreceptor gap junctions.

Ultimately, a combination of many or all of these possibilities could be contributing to cone degeneration after rod death in RP. Until the mechanism is more thoroughly derived, it is unlikely that therapeutic strategies to stall cone death will be successful long term.

1.2.2 Cone dystrophies

1.2.2.1 Age-related macular degeneration

Age-related macular degeneration (AMD; OMIM #603075) is a common cause of blindness in older individuals, and results from the degeneration of cone photoreceptor cells within the cone-dense region of the retina, known as the macula. AMD is characterized by progressive loss of central vision and accumulation of lipid deposits called drusen beneath the retina, which appear as yellow flecks on Fundus. There are two forms of AMD – dry AMD and wet AMD. Dry AMD is the most common form of AMD, and is characterized by geographic atrophy that results from the degeneration of RPE, photoreceptors, and choroid. Wet AMD is characterized by choroidal neovascularization. The new vessels are often fragile and prone to leaking or breaking, which can lead to blood deposition and scarring. Wet AMD can be treated with drugs that target vascular endothelial growth factor and prevent further neovascularization, but there are no effective treatments for dry AMD.

AMD is a complex disorder, and interactions between both genetic and environmental factors contribute to risk of developing AMD. Environmental factors such as smoking, increasing age, previous cataract surgery, and high body mass index can increase risk of developing AMD [21]. The innate immune system, or the complement system, plays a role in AMD; this was first suggested when components of the complement system were found to accumulate within drusen [22-24]. Mutations in complement factor H (CFH) were the first genetic links to AMD that were deciphered [25-27]. Since then, mutations in other complement system members have also been linked to AMD susceptibility, including *complement factor I* (*CFI*), *complement factor B* (*CFB*), *complement component 3* (*C3*), and *complement component 2* (*C2*) [28-34]. It has been suggested that loss of complement regulation in the RPE cells could result in inflammation and compromise the RPE [35]. The RPE is necessary for the support of photoreceptors; deterioration of RPE results in photoreceptor cell death.

1.3 Therapies to treat blindness

Currently, there are no effective treatments to prevent or reverse photoreceptor degeneration. However, there are promising therapeutic strategies being developed and optimized in animal models and clinical trials to prevent or reverse photoreceptor degeneration. While a lot of work focuses on designing disease therapies, this thesis work can be applied to disease models and therapies to aid in gauging therapy success.

1.3.1 Gene Therapy

In cases where disease is caused by loss-of-function mutations, viral vector-mediated gene therapy can be used to add a functional copy of a gene. Gene therapy involves introducing a functional copy of a gene via a viral vector, such as adeno-associated viral (AAV) vectors. These particular vectors have gained popularity because

they are able to transduce terminally differentiated/non-dividing cells, and are therefore ideal for use in the mature retina, where cellular turnover is low. Additionally, the AAV used in gene therapy cannot integrate into the host genome, reducing the possibility of insertion into important regulatory or protein coding sequences. However, large genes cannot be packaged into AAV, as its capacity is less than 5kb, and so it is only appropriate for smaller genes. AAV was found to successfully and safely transduce photoreceptor and RPE cells in mice, making AAV a candidate for retinal gene therapy development and optimization [36].

Another promising vector that is gaining popularity for use in gene therapy is the equine infectious anemia virus (EIAV). EIAV is a lentivirus that has a higher capacity than AAV; it can package up to 8kb [37]. EIAV is an integrating virus, meaning that it is incorporated into the genome of the host cell. This allows for stable long-term expression of the introduced gene, but also poses the risk of integration into necessary genes or disruption of proto-oncogenes. Promisingly, though, EIAV has not yet been observed to insert into area of the genome that cause gene disruption or oncogenesis. Another benefit of EIAV is that it is non-immunogenic, and is therefore unlikely to trigger an immune response or inflammation. EIAV has been shown to be safe and has been used in clinical trials to treat Parkinson's disease [38], and is now being tailored for use in retinal gene therapy. In the *ATP-blinding cassette, subfamily 4a* (*Abca4*) knockout mouse, a model for a cone dystrophy called Stargardt disease, EIAV was able to successfully introduce a functional copy of *Abca4* [39]. EIAV was also able to transduce rods and cones in adult macaque retina, and thus seems promising for treatment of photoreceptor degenerative diseases in human patients [40].

Gene therapy trials on human patients with retinal diseases using AAV have had some reported success [41-45], but results have been inconsistent. Additionally, there was

foveal thinning and retinal detachment in some of the patients of early trials. New methods of vector delivery are used to help limit this, by detaching the retina at the injection site, though retinal thinning and detachment are still risks of the procedure. Ultimately, animal models must be used to develop new therapies and to optimize current strategies.

Gene therapy has the potential to reverse vision loss to some extent. Cells that are dysfunctional, but still alive, could regain some function post transfection. For example, in retinitis pigmentosa caused by loss-of-function alleles, the cells could still be thriving but dysfunctional, and introduction of a functional copy of the gene could allow for some vision recovery. However, the amount of functional recovery of sight may not be substantial, and photoreceptor degeneration may continue regardless due to changes that may exist in the microenvironment of the degenerating retina. There is nonetheless potential to use viral transfection to change cell fate or induce stem cell fates and reverse vision loss.

1.3.2 Stem cell transplantation

Transplantation of photoreceptor precursor cells is a promising therapy to replace lost photoreceptors. Photoreceptor precursor cells have only a limited number of cellular divisions, unlike stem cells which can divide continually, which reduces the concern of introduced cells becoming cancerous. The photoreceptor precursor cells can be derived from various sources. Embryonic stem cells (ESCs) are pluripotent stem cells, meaning that they are able to differentiate into any cell type that makes up the body, and are collected from embryos. However, there are several issues surrounding ESCs, including that the patient would likely have to undergo lifelong immunosuppressive therapy, the difficulty obtaining ESCs, and ethical concerns surrounding ESC use in humans. Thus,

induced pluripotent stem cells (iPSCs) are an appealing option for stem cell transplantation. IPSCs are stem cells that can be generated using differentiated tissue, such as fibroblasts, by virally transducing the cells to express specific transcription factors to induce a stem cell fate [46-48]. A major benefit of iPSCs is that cells can be collected from the patient, which reduces the need for immunosuppressant therapy and makes rejection less likely.

Both ESCs and iPSCs can differentiate and self-organize into eye cup-like structures, or retinal organoids [49-52]. These 3-D structures develop many retinal cell types (though the degree to which they mature can vary), including RPE, photoreceptors, bipolar cells, and horizontal cells. However, while retinal ganglion and amacrine cells can differentiate, they subsequently degenerate, and the RPE cells clump together and do not form an even sheet across the organoid [53]. Determining which cells at which developmental stage are appropriate for transplant is crucial, as the introduced cells must not only survive in their new environment, but also find their appropriate positions within the retina, form connections, and perform necessary functions. Donor post-mitotic photoreceptor precursor cells have been determined the most successful at surviving, localizing to the ONL, and appear to integrate into the recipient neural retina [54-59]. Integration is difficult to study, however, as successful integration involves the cells not only moving to the correct location, but also generating the necessary connections, and communicating effectively with surrounding cells. It is difficult to assess whether introduced cells have generated the appropriate connections with surrounding cells, and whether these connections are producing a functional output.

One major benefit of cellular transplantation as a therapeutic technique is that it can be applied to many different photoreceptor degenerative diseases, including extremely heterogeneous diseases, such as retinitis pigmentosa or age-related macular

degeneration. Nonetheless, donor cell selection must be personalized to match the recipient's needs. This could involve selecting cells from a pre-existing pool of potential donor cells categorized by specific genetic markers, or could involve using the patient's own cells. The latter could be used in combination with gene editing or gene therapy techniques to remove deleterious mutations or add a functional gene copy from the patient-derived donor cells in order to increase survival.

Ultimately, stem cell transplantation is an appealing and promising strategy to treat blindness and restore vision, but further research is needed to determine whether transplanted cells are able to effectively communicate with the host retina and produce a functional output. Integration success of introduced retinal progenitor cells has been difficult to analyze and the range of reported success stretches from less than 1% cellular integration to 30% [49, 54-61]. However, these results have been confounded by the discovery of material transfer. In mice, donor photoreceptor precursor cells and host retinal cells are able to transfer material, which allows for host cells to express donor cell markers and vice versa [62-65]. Therefore, the success rates of retinal progenitor cell integration studies have been over-reported.

1.3.3 Clustered regularly interspaced short palindromic repeat (CRISPR)/CRISPR associated protein (Cas) gene editing

CRISPR/Cas is an adaptive immune system found in prokaryotes to protect against foreign genetic material, such as DNA introduced by phages, whereby Cas nuclease digests the exogenous DNA [66]. The system has been modified to allow for targeted editing of genomes [67]. This works by generation of a synthetic guide RNA (gRNA), which creates a complex with Cas9, a Cas protein derived from *Streptococcus pyogenes*. The gRNA help guide the Cas nuclease to the corresponding target sequence, where it

cuts the DNA. The DNA can be repaired via non-homologous end joining, which typically introduces insertions or deletions, or homology-directed repair, which involves also introducing a nucleotide template that includes the desired changes that the researcher wants to be added to the endogenous DNA. The CRISPR/Cas9 system has become a favourable gene editing method for generating animal models of disease by introducing mutations to specific genes.

The CRISPR/Cas9 system has promising implications for treating blindness, particularly in combination with other therapeutic strategies. The generation of human iPSCs has been promising for the production of retinal stem cells, but limitations surrounding this methodology include the potential for rejection in cases where the introduced donor cells are not patient-derived, and, when patient-derived cells are used, the cells contain the disease-causing mutation and therefore could still progress into a disease state. Combining iPSC technology with CRISPR/Cas9 gene editing allows for the patients' cells to be used to create retinal progenitor cells that no longer carry the deleterious mutation. Additionally, as the iPSC cells are outside of the body, the population could also be sampled and tested for off-target cutting.

Recently, AAV delivery has been utilized to introduce CRISPR/Cas9 into mouse retinal cells to remove genes [68, 69]. The method successfully removed fluorescent protein expression from transgenic mouse retina [68, 69]. AAV delivered CRISPR/Cas9 was also used to target a transcription factor, neural retina-specific leucine zipper protein (*Nrl*) [68], which is known to induce rod fate in photoreceptors [70]. The loss of *Nrl* in mature rods caused the cells to take on some cone-like features, and slowed photoreceptor degeneration in three different mouse models of retinitis pigmentosa [68]. This provides a unique opportunity for therapies in the future – it may be possible to slow or halt photoreceptor degeneration by manipulating photoreceptor features, such as by

making rods more cone-like in rod dystrophies, where rods typically degenerate and cones usually persist.

Despite the potential of the CRISPR/Cas9 system, it still has some notable drawbacks. It is difficult to assess the off-target activity of CRISPR/Cas9, and its off-target activity could result in disruption of necessary genes or activation of oncogenes. While using CRISPR/Cas9 on cultured patient iPSCs allows for sampling and more thorough assessment of off-target activity, it is difficult to effectively determine whether non-target sequences have been manipulated without thorough sequencing, which is time consuming and expensive. The method of CRISPR/Cas delivery to the cells also must be considered. Delivery to intact retinal tissue using viral vector could pose issue, as integration of the Cas gene into the host cell's genomic DNA could result in rogue Cas9 expression and the modification of non-target genes.

1.4 Zebrafish as a model for investigating retinal connectivity and degeneration/regeneration

Zebrafish are an ideal model for retinal development and connectivity. The zebrafish retina is conserved to the mammalian retina in terms of development, structure, and function. Zebrafish also undergo external fertilization, which allows for easy monitoring of the rapidly developing zebrafish visual system. Eye field patterning begins at 28 hours post fertilization (hpf), and the developing zebrafish eye begins expressing opsin genes as early as 51 hours post fertilization [71]. At 5 days post fertilization (dpf), zebrafish can respond to visual stimuli [72]. This means that visually-mediated behaviours can be assessed early in the developing zebrafish.

The zebrafish retina is cone-rich and consists of four cone photoreceptor subtypes – UV-sensitive (*sws1* gene), blue-sensitive (*sws2* gene), red-sensitive (*lws1* and *lws2*

genes), and green-sensitive (*rh2-1, rh2-2, rh2-3*, and *rh2-4* genes) [73-78]. The zebrafish blue and UV cones are independent single cones, while the red and green cones exist as a physically joined double cone. The cone photoreceptors in the zebrafish retina are organized into a predictable row mosaic [78-81].

1.4.1 Photoreceptor mosaic

A photoreceptor mosaic is the organization of the photoreceptors across the retina. Some mosaics are stochastic, meaning that the organization of the photoreceptor cells is random and does not follow a recognizable pattern, while others are organized [82]. All or only a subset of photoreceptor subtypes may participate in an organized mosaic, while the other (non-participating) photoreceptors distribute stochastically across the retina. Mosaics can also be organized regionally, where photoreceptors are in specific densities in particular retinal regions, but the organization within the region is stochastic. Examples of regionalized photoreceptor mosaics include the human mosaic and the mouse mosaic. Appreciating how the zebrafish mosaic is similar and different from the human mosaic is important, especially when it comes to relating information gleaned from zebrafish to the human system.

Humans have a regionalized mosaic, where photoreceptor subtypes are found in specific regions in particular densities (Figure 2). Humans possess four photoreceptor types in their retinas: rods, blue-, green, and red-sensitive cones. The periphery of the human retina is very rod-dense with blue, red, and green cones interspersed. Near the centre of the human retina is a cone-dense macula, which contains packed red and green cones (Figure 2). In Fundus images, the macula appears as a yellow spot in the retina. The macula can be further subdivided into the parafovea, which is the periphery of the macula where retinal ganglion cell layer has 2-4 RGCs layered, the perifovea, which is the

extremely cone-dense centre of the macula where RGC layer has 5 or more layers of RGCs, and the fovea. The fovea is an indentation caused by the downstream neurons moving to the side, allowing for light to reach the cones with little interference.

Mice, like humans, have a regionalized mosaic, where the distribution of blue and green cones is along a gradient across the retina (Figure 2). The mouse retina possesses cones that express both blue and green opsin at varying levels – this expression of two opsins within a single cone does not occur in the mature human retina. Mice are nocturnal, and as a result have a rod-dominant retina with comparatively few cones. There is no cone-dense region, or area centralis, within the mouse retina.

Adult zebrafish, conversely, have an organized row mosaic [78-81]. Cone photoreceptors are predictably arranged in rows across the zebrafish retina, where UV and blue cones alternate within their row and red/green double cones alternate in their row, with rods packed between (Figure 2). The consistent structure of the photoreceptor mosaic means that the photoreceptors have predictable neighbours, which can be utilized for investigation of photoreceptor connectivity and factors contributing to retinal patterning. Unlike the adults, larval zebrafish do not have an organized row mosaic and the proportion of cones differs from that of the adults [78]. Rather, the larval mosaic appears more regionalized, with tightly packed cones evenly distributed and rods existing primarily in the ventral retina. As the fish grows, additional photoreceptors are added at the periphery of the retina, and the retina transitions to the row mosaic. Many fish have precisely organized cone mosaics, but the benefits and purpose of these mosaics is still uncertain.

1.4.2 Retinal connectivity in zebrafish

Light information undergoes extensive processing before it reaches the brain. Lateral interactions between cells in the retina play key roles in early visual processing. Indeed, lateral inhibition by interneurons in the outer retina contributes to edge detection, contrast enhancement, and colour opponency, and lateral photoreceptor-photoreceptor interactions are speculated to play a role in enhancement of visual acuity and reduction of background noise under specific light conditions [83-89].

1.4.2.1 Horizontal cell connectivity

Horizontal cells (HCs) are located in the inner nuclear layer, and extend processes into the outer plexiform layer to contact photoreceptor synaptic terminals. HCs provide inhibitory feedback to the photoreceptor cells, and are able to modulate cone output in this manner. By summating the information from numerous photoreceptors across space, the HCs are able to provide information for contrast enhancement, colour constancy, and colour opponency, which is the idea that colour information from rods and cones is processed in an antagonistic manner [90, 91]. More recently, HC feedback was found to be capable of acting on a small scale, such as between a single HC connection and photoreceptor, suggesting that horizontal cells can influence both local and global light information processing [84, 92, 93].

The mammalian retina typically possesses two types of HCs, with the exception of the extremely rod-dominant mouse and rat retina, which only have a single horizontal cell type [94]. The primate retina possesses HI and HII HCs. HI cells are axon-bearing, with their cell dendrites contacting red and green cones and its axon terminal connecting to rods [95-97]. HII cells lack an axon and their dendritic contacts are predominantly with blue cones but still innervate some red and green cones [95-99]. It is believed that

HII HCs assess green and red cone input and provide lateral inhibition to the blue cones. This has the potential to generate colour opponency in the visual system.

The zebrafish retina contains four types of HCs: H1, H2, H3, and H4 HCs, all of which have distinct morphologies and specific photoreceptor connectivity partners. H1 HCs have axons and connect with all cone types; H2 HCs have axons and contact green, blue, and UV cones; H3 HCs also have axons and contact exclusively blue and UV cones; and H4 HCs, which are the only axonless HC in the zebrafish retina, contact UV cones and is the only HC that contacts rods [100-102].

HCs are a source of neural plasticity in the retina. H3 HCs have been found to connect with UV and blue cones in a 5:1 synapse ratio in the larval zebrafish retina. After the targeted ablation of UV cones and prevention of UV cone regeneration (via the nitroreductase mechanism of cellular ablation, see 1.4.4.1), the H3 horizontal cell primary connection partner, H3 horizontal cells generated additional synapses with blue cones and also connected with atypical partners [103]. Conversely, in a *lots-of-rods* (*lor*) mutant retina, which has an abnormally high density of rods and few UV cones, H3 horizontal cells made additional connections with blue cones but did not make aberrant connections with other photoreceptor types [104]. Therefore, it seems as though H3 horizontal cells respond to a lack of UV cones in development by creating additional connections with blue cones. It was also discovered that UV cone activity mediates the ratio of UV:blue cone contacts made by H3 horizontal cells. Tetanus toxin inhibits synaptic transmission by interfering with exocytosis. After expressing tetanus toxin in UV cones, blue cones, or both, H3 horizontal cell blue cone contacts were increased only when UV cone transmission was disrupted [104].

1.4.2.2 Photoreceptor-photoreceptor connectivity

Photoreceptor connectivity is often investigated in terms of connections between photoreceptor cells and their downstream cellular contacts, bipolar and horizontal cells. However, photoreceptors make connections with other photoreceptors, via fine processes called telodendria. Telodendria are conserved structure of vertebrate photoreceptors. While telodendria were first noted as common features of cones in the 19th century [105, 106], this network of photoreceptor-photoreceptor connections has been largely overlooked, and the functional consequence of these connections is speculative at best. Photoreceptors use telodendria to exchange electrical information via gap junctions, and electrophysiology studies found that when a photoreceptor was stimulated, the photoreceptors that it was coupled with also had a response [107-112]. It therefore seems that photoreceptors are using telodendria to communicate and this could be influencing the light information processing early on. Whether signals sent through telodendria are modified based on horizontal cell feedback is unknown, though there is potential for horizontal cell inhibition to influence how the photoreceptor cells communicate with one another. Photoreceptor-photoreceptor connectivity in the zebrafish retina has not been characterized until now.

1.4.3 Regeneration of retinal neurons

The mature human retina has a very limited capacity to replace lost neurons, meaning that loss of any retinal neurons is irreversible and can lead to vision impairment. Zebrafish, conversely, are able to replace retinal neurons via two distinct regenerative pools: the ciliary marginal zone and Müller glia. Zebrafish thus provide a unique opportunity to investigate retinal stem cell activation, differentiation, and integration [113-124].

1.4.3.1 Ciliary marginal zone

The ciliary marginal zone (CMZ) is a pool of retinal stem cells located at the periphery of the retina. In many species, this pool becomes inactive once the retina has matured. However, in most vertebrates (zebrafish and other species that undergo indeterminate growth), the CMZ self-renews and is constantly adding new retinal neurons at the edges of the retina. The CMZ contains both retinal stem cells, which can continue to divide indeterminately and stay in close contact with the CMZ, and retinal progenitor cells, which are only able to divide a certain number of times and can lose contact with the CMZ as differentiation occurs. Retinal stem cells sit in the edges of the CMZ, and typically undergo asymmetrical division to produce a retinal stem cell and a retina progenitor cell [125].

1.4.3.2 Endogenous stem cells (Müller glia)

Müller glia are support cells that regulate ion levels, mediate uptake and degradation of neurotransmitters, removal of cellular debris, and insulate receptors and neurons. In zebrafish and other teleost fishes, these cells also act as endogenous stem cells by undergoing de-differentiation, proliferation, and specification [118, 121, 122, 126]. Zebrafish Müller glia undergo asymmetrical division, and therefore can replenish lost retinal neurons while self-renewing, allowing for the persistence of the stem cell pool [121].

As Müller glia are present within the human retina, there is much interest surrounding how the stem cell behaviour of Müller glia is activated and whether mammalian Müller glia could be re-programmed to allow for stem cell fate and neurogenesis within the mature human retina. Human Müller glia respond to damage and can have stem cell characteristics, but do not naturally undergo neurogenesis *in vivo*

[127, 128]. In culture, human Müller glia treated with growth and differentiation factors can take on stem cell-like characteristics and differentiate into rod-like cells, expressing photoreceptor markers [129]. Rod photoreceptors derived from human Müller glia cultures have successfully been introduced into a rat model of retinitis pigmentosa and were able to migrate into the ONL and restore some visual function [130].

1.4.4 Zebrafish as a model for photoreceptor degeneration/regeneration

Zebrafish are able to regenerate retinal neurons, and are thus of interest for studying regeneration. In order to study regenerative responses, the retina must first be lesioned. There are various acute and chronic methodologies that allow for the destruction of retinal neurons and investigation of neuronal regeneration [118].

1.4.4.1 Nitroreductase-mediated targeted cell ablation

Nitroreductase (NTR) is an enzyme originally found in bacteria, which can reduce otherwise inert prodrugs, such as metronidazole (MTZ), into DNA cross-linking agents [131]. This process allows for the specific ablation of cells expressing nitroreductase. The major benefit of this particular cellular ablation mechanism is its specificity; only cells expressing NTR should undergo apoptosis, as the prodrug is apparently harmless to healthy cells. Indeed, the specificity of this method has been demonstrated in transgenic zebrafish expressing NTR in certain types of retinal cells; there does not appear to be a toxic bystander effect that is damaging non-target (non-NTR expressing) cells post ablation of photoreceptor subtypes in the retina [114, 119, 132]. The NTR mechanism of ablation is thus one of the few methods that allows for ablation of targeted cell subtypes. Additionally, as NTR-fluorescent protein fusions have been made, the degeneration of target cells can be followed, and, where possible, regeneration of these cells can also be observed. It is also possible to delay, or prevent, the regeneration of the target cell type by

continued treatment with MTZ, since regenerating cells will undergo apoptosis once they begin to express NTR. However, this ablation method involves generating transgenic animals that express NTR under specific promoters, which may not be feasible in non-model animal systems or for targeting cell populations that are genetically complex.

Intriguingly, ablation of specific cell subtypes can reveal thresholds for triggering regenerative responses. In the larval zebrafish retina, NTR ablation of blue cones stimulated negligible amounts of regeneration – however, simultaneously ablating both blue and red cones using the NTR mechanism successfully induced robust regeneration [103]. Conversely, ablating UV cones was successful in stimulating a regenerative response [103, 119].

1.4.4.2 Light ablation

Light ablation allows for the ablation of photoreceptors and leaves the remaining neural retina relatively intact [123, 133-135]. One drawback of light ablation is that it typically causes generalized destruction of many different photoreceptor types. Though some optimization has been successfully undertaken to ablate specific subtypes of cones using light of a particular wavelength, this is difficult to achieve. Post light ablation in fish, a robust regenerative response occurs, generated largely by proliferation of Müller glia [122].

1.4.4.3 Surgical lesion

Surgical removal of part or the entire retina has been assessed in teleosts and whether these methods stimulate a regenerative response [136]. Removing the retina in its entirety prevents regeneration, likely due to removal of stem cell pools, but leaving even small amounts of retina leads to regeneration. Surgical disruption of the retina is thus useful to study widespread regeneration of the retina, but not for the isolated

investigation of factors involved in regeneration of specific cell types. After surgical lesioning, the retina is regenerated such that the proportions of neuron types are roughly the same as before [113, 136, 137]. Intriguingly, the cone mosaic is not re-formed after photoreceptor regeneration [138].

1.4.4.4 Toxic lesion

Lesion using a neurotoxin can be achieved by administration of ouabain. Ouabain acts by inhibiting the Na+/K+ ATPase, and is administered using intravitreal injection, and the dosage used determines the retinal layers that are affected – high doses can penetrate far into the retina, causing destruction of many cell types, while lower doses are unable to penetrate as far, and ablation is therefore restricted to the inner retinal layers [116, 139]. However, this method cannot easily be limited to only one cell type. In zebrafish, ouabain has been used successfully to ablate retinal neurons, and this method stimulates a regenerative response [116].

1.4.4.5 Excess fluorescent protein expression

1.4.4.5.1 Rod degeneration model

All the aforementioned mechanisms of retinal neuron ablation are acute lesions, and few zebrafish models of chronic photoreceptor degeneration exist. The XOPS:mCFP transgenic zebrafish line expresses cyan fluorescent protein (CFP) under the *Xenopus* rhodopsin promoter (*XOPS*) [140]. There is an overabundance of CFP produced, leading to toxicity that causes rod degeneration. In this model, the pool of rod precursors expands in the adult retina. Intriguingly, there was no sign of cone death, despite rod loss [140] – this differs from what is observed in humans with retinitis pigmentosa, where cone degeneration follows rod degeneration. This reason for this is unclear, though could be

due to the cone-rich environment of the zebrafish retina, compared to the rod-rich environment of the human/mammalian retina.

1.5 Purpose of study/objectives

The objective of this project was to characterize photoreceptor telodendria morphology and connectivity in the zebrafish retina at different life stages. Telodendria are conserved structures of vertebrate photoreceptors, zebrafish provide the opportunity to investigate telodendria using fluorescent protein expression in specific photoreceptor subtypes. Historically, telodendria were visualized using stains, dye injections, or antibody labelling – the novel use of fluorescent protein expression to visualize telodendria increases the ease of structure visualization. Zebrafish also have many tools available to manipulate photoreceptors, including mutants with altered photoreceptor proportions and photoreceptor cell ablation mechanisms.

The first aim was to characterize the morphology and connectivity of short wavelength cones in the highly organized adult zebrafish retina. As the adult zebrafish retina is organized into a row mosaic, the connectivity of the telodendria was expected to be relatively consistent between cells of the same subtype.

The second aim was to determine how early telodendria can be observed in the developing retina, and to investigate whether telodendria characteristics change between the larval and adult zebrafish retinas. The larval retina lacks the structured row mosaic of the adult retina and possesses different proportions of photoreceptors, and this different environment could influence telodendria connectivity.

The third aim broadly sought to disrupt the photoreceptors in various ways that might reveal new information about telodendria development, maintenance, or physiology. For example, one manipulation was designed to assess whether telodendria

were a source of retinal plasticity by ablating blue cones and investigating UV cone telodendria in the larval retina. Past work in our lab found that after blue cone ablation, visually-mediated behaviour recovered rapidly to baseline levels in 24 hours post ablation, despite lack of physical regeneration [132]. Telodendria were a potential source of this plasticity, as the non-ablated short wavelength cone (UV cones) may be rewiring and compensating for blue cone loss.

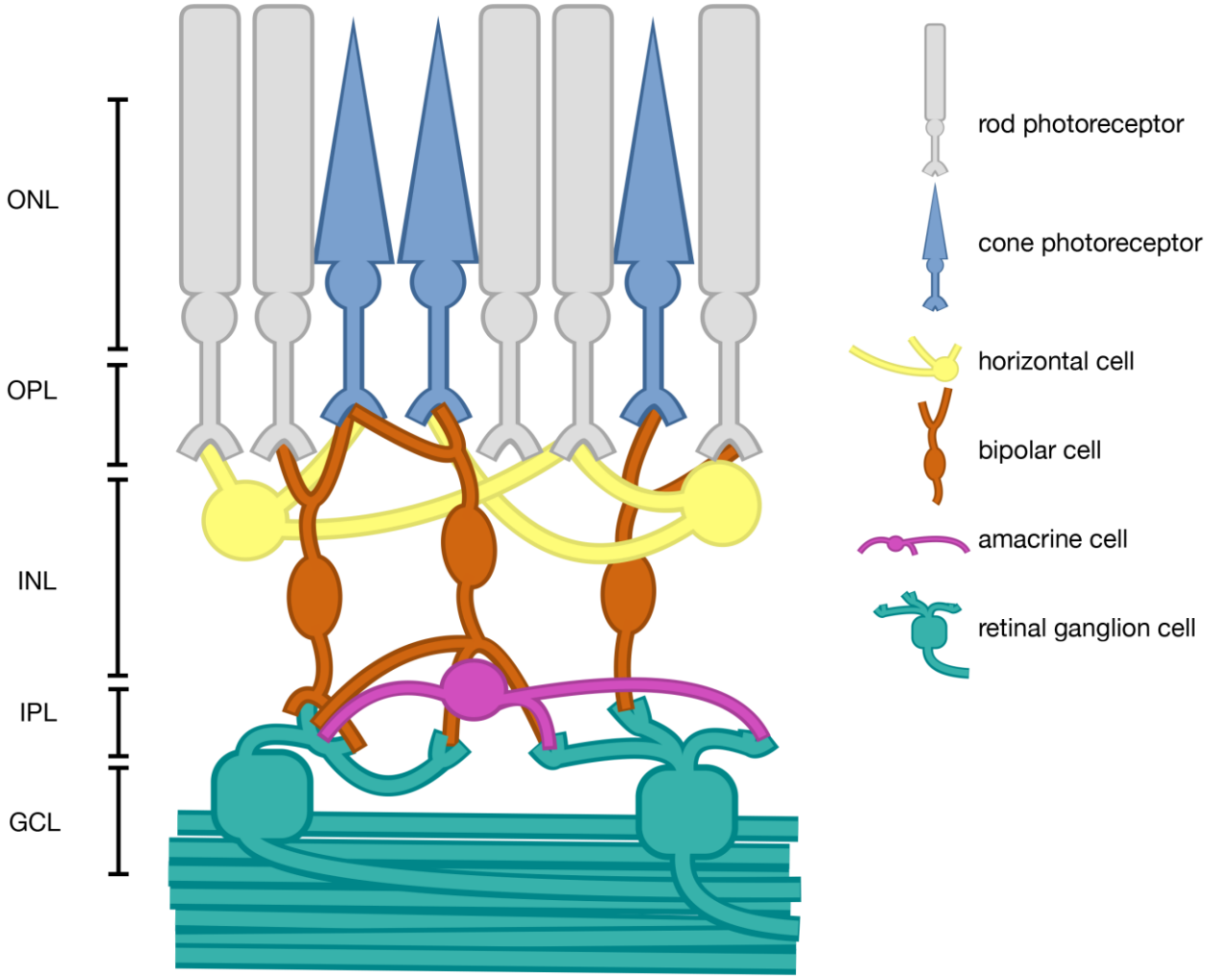
ONL
OPL
INL
IPL
GCL
rod photoreceptor
cone photoreceptor
horizontal cell
bipolar cell
amacrine cell
retinal ganglion cell

Figure 1. Organization of the neural retina.

At the back of the eye are the light-detecting cells, known as photoreceptors, in the outer nuclear layer (ONL). There are two types of photoreceptor cells: rods, which are sensitive to dim-light and responsible for vision in low light conditions, and cones, which are sensitive to specific wavelengths of light and responsible for daytime and colour vision. The outer plexiform layer (OPL) is where the photoreceptors synapse with downstream neurons, such as horizontal cells and bipolar cells. The inner nuclear layer (INL) contains the cell bodies of the horizontal cells, bipolar cells, and amacrine cells. The inner plexiform layer (IPL) is where bipolar and amacrine cells make contacts with the retinal ganglion cells. The ganglion cell layer (GCL) contains the retinal ganglion cells, the axons of which form the nerve fibre layer and converge to form the optic nerve, which exits the eye and connects to the brain.

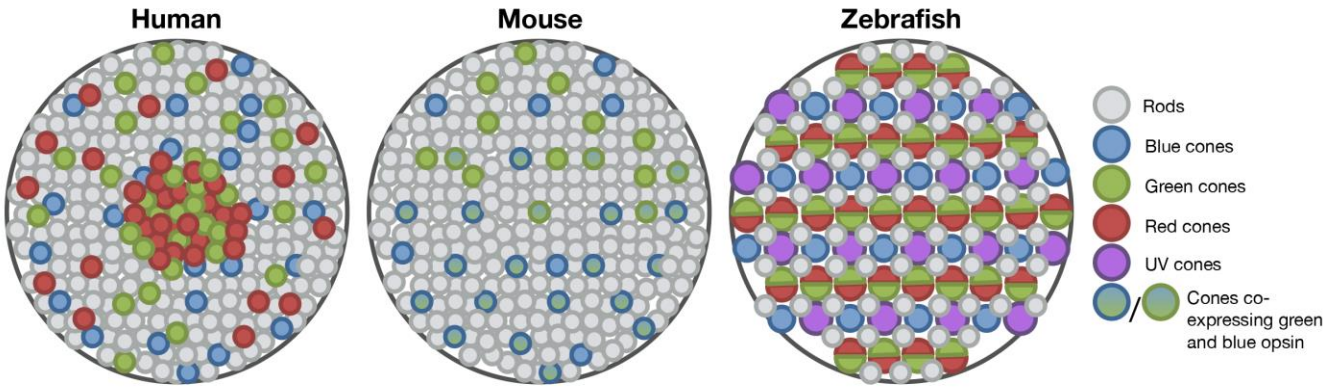

Figure 2. Photoreceptor mosaics of the human, mouse, and zebrafish retina. The human retina is organized regionally, and contains an abundance of rods around the retinal periphery with cone interspersed. The human retina has three types of cones: red, blue, and green cones. Towards the centre of the retina is the cone-dense macula. The mouse retina is also regionalized, but only expresses two opsins (blue and green). The mouse retina is extremely rod-rich, with cones studded throughout, and contains cones that express more than one cone opsin. There are more blue cones in the ventral retina, with more green cones in the dorsal retina. Adult zebrafish possess a row mosaic, wherein its cones (UV, blue, green, and red) are highly organized.

2 CONNECTIVITY OF PHOTORECEPTOR TELODENDRIA IN THE ZEBRAFISH RETINA

2.1 Introduction

The first synapse of the vertebrate visual system relays information from the photoreceptors to bipolar cells, and is serviced by horizontal cells that connect laterally amongst these adjacent synapses. The latter provides feedback amongst the neighbouring photoreceptors, which enables the comparison and amplification of signals to improve resolution of visual stimuli and detection of their various characters such as edges, sizes, and movements. Similarly, such feedback underpins comparison between spectral subclasses of cones and enables discrimination of wavelengths and colour constancy. The mechanisms of this lateral inhibition continue to be debated [87, 88, 141]. Perhaps prior to this remarkable first synapse, however, adjacent photoreceptors are also coupled directly via telodendria. Telodendria are projections that originate from the photoreceptor pedicle and form gap junctions with other photoreceptors [89, 142-144]. Considering the vast and celebrated literature describing the morphology and connectivity of the outer retina, it is notable how little attention has been given to the role(s) of photoreceptor telodendria. The lack of attention regarding telodendria is likely due to the technical difficulty in defining their morphology amongst the many cellular processes that appear in ultrastructural analysis. Regardless, the pattern of direct coupling between photoreceptors, and whether it might serve to differentially couple certain photoreceptor subtypes, is expected to substantially impact the initial steps of visual signal processing.

Telodendria were first observed in the human retina, and noted to be a common feature of photoreceptors in the 19th century [105, 106]. Since then, photoreceptor

telodendria have been reported in many vertebrates, such as reptiles [83, 85, 86, 108, 111, 145-150], amphibians [151-153], fish [89, 143, 154-156] and mammals [110, 142, 157-159], including non-human primates [144, 160-162]. It was noted that these photoreceptor projections were forming gap junctions with their targets based on inferences from ultrastructural analysis, the presence of connexin, and electrophysiological assessment, suggesting that photoreceptors are indeed using these processes to communicate with other photoreceptors [83, 86, 89, 107, 108, 110, 142-144, 146-150, 152, 154, 157, 158, 160]. The function of telodendrial connections remains ambiguous, though they are speculatively thought to improve cone sensitivity and play a role in specific light situations (such as crepuscular vision) to reduce background and increase visual acuity [110, 144, 158, 161] and reduce signal-to-noise [109, 112, 151]. The anatomy and organization of telodendria has been challenging to define due to their small size and tortuous complexity within the photoreceptor pedicles and outer plexiform layer (OPL); describing the organization/connectivity of telodendria is expected to inspire new hypotheses about their physiological contribution to vision.

Zebrafish provide a unique opportunity to investigate cone photoreceptor telodendria in detail. The tetrachromatic zebrafish retina possesses an abundance of cone photoreceptors, akin to the cone-rich macula of humans. Zebrafish have cones that are sensitive to ultraviolet (*sws1* gene, homologue of the human blue opsin), blue (*sws2* gene), red (*lws1* and *lws2* genes), or green (*rh2-1, rh2-2, rh2-3*, and *rh2-4* genes) light [73-77]. Cones in the retina of adult zebrafish are organized into a highly structured row mosaic (Figure 2; Figure 3) [79-81, 119], though the mosaic in the larval retina is less pronounced [78]. This organized lattice of cones can aid in characterization of photoreceptor connectivity, as the photoreceptors have neighbours of a predictable subtype.

Historically, the visualization of telodendria has been accomplished via electron microscopy, dye injection, or fluorescent antibody labeling [86, 111, 142, 144, 154, 156, 157, 160]. In zebrafish, transgenesis technology permits the expression of fluorescent proteins under cone-specific promoters, which provides the opportunity for visualization and characterization of telodendria. Here, we explore the telodendric connectivity of UV and blue cones in unperturbed adult and larval retina expressing fluorescent markers within UV and blue cones. We assessed UV cone telodendria in mutant larval retina wherein there is an atypically small proportion of UV cones and an abundance of rod photoreceptors. This could give insight into factors that are necessary for telodendric pathfinding; with fewer neighbouring UV cones, the behaviour of the UV cone telodendria could be altered, due to absence of putative factors limiting the field size of neuronal projections. Additionally, we characterized rod telodendria in the larval retina.

Telodendria are a potential source of neural plasticity, and may change in connectivity after retinal manipulation. Previously, it was observed that the optomotor response (OMR) in larval zebrafish was abolished immediately after targeted ablation of UV or blue cones, but quickly recovered to baseline after loss of blue cones [132]. OMR is an innate visually mediated behaviour, whereby the zebrafish larvae swim in the direction of perceived motion. To investigate how OMR changed after loss of specific cone types, an optimized low-contrast blue and red bar stimulus that the larvae were unable to respond to after short wavelength cone loss was utilized [132]. The underlying mechanism leading to this rapid recovery post blue cone death has been elusive, but it is possible that the other short wavelength cone (UV cones) is able to compensate for the loss of blue cones, and this compensation may be visible in the number of telodendric connections made by UV cones. We assessed the number of UV cone telodendria after targeted ablation of blue cones in the larval retina.

In summary, we describe the morphology of blue and UV cone telodendria in mature and developing zebrafish retina, as well as rods in the larval retina. Ultimately, characterizing telodendric patterns further elaborates on the complex vertebrate retina connectome and has potential to aid in addressing questions of photoreceptor integration during development and following stem cell transplantation.

2.2 Methods

2.2.1 Animal ethics

The Animal Care and Use Committee: BioSciences (an Institutional Animal Care and Use Committee at the University of Alberta, operating under the Canadian Council on Animal Care) approved this study under protocol AUP00000077.

2.2.2 Zebrafish care

Zebrafish embryos used in experiments were harvested and transferred into and grown in E3 media [163]. All larvae were treated with 1-phenol-2-thiourea (PTU) mixed with E3 media at 6-8 hours after fertilization to prevent the production of melanin pigment and grown at 28°C. E3 media was changed daily. After 6 days post fertilization (dpf), larvae are fed powdered fish fry food.

Adult zebrafish were maintained according to standard procedures [163] at 28°C in light-controlled conditions (14L:10D). The zebrafish are fed twice a day; in the morning, they are fed trout chow, and in the evening, they are fed brine shrimp. A description of the zebrafish lines used is provided in Table 1.

2.2.3 Tissue dissection and fixation

Larvae were euthanized with MS-222 and transferred into 4% paraformaldehyde in 0.1M phosphate buffer + 5% sucrose, pH 7.4 (PFA). Larvae were fixed overnight at 4°C.

After fixation, the PFA was removed and the larvae were washed and stored in 1x phosphate buffered saline, pH 7.4 (PBS) + 0.1% Tween 20 (PBSTw) until use.

For retinal dissection, larvae were transferred into 50% glycerol and placed on a slide. Tungsten wires sharpened into microscalpels [164] were used to remove the lens from the eye, and eyes were positioned such that the photoreceptors could be imaged through the sclera.

In preparation for retinal dissection, adult fish were dark-adapted for at least eight hours to allow for the retinal pigment epithelium (RPE) to pull away from the retina. This occurs in the dark, as during the light the photoreceptors are undergoing rapid OS shedding, which is absorbed by the RPE. All dissections were conducted in a dark room, under red light to prevent the RPE from re-adhering to the retina. Dissections took place in the early afternoon, between noon-2pm, or, for the nighttime dissections, between midnight-2am.

Adult zebrafish were euthanized with MS-222 and underwent cervical dislocation before undergoing dissection. Whole eyes were removed, placed in PBSTw, and the retina was dissected out using forceps. The tissue was transferred into 1.5mL microfuge tubes (one retina per tube) and fixed at room temperature for 45 minutes in 4% PFA. The lens was left attached to the retina during fixation when possible, to prevent the retina from folding or wrinkling. After fixation, retinas were transferred into 50% glycerol/PBS, and allowed to equilibrate for 30 minutes. The 50% glycerol was then replaced and the retinas were stored until use.

To mount for microscopy, the retinas were positioned (in 50% glycerol/PBS) on a glass slide, the lens removed, and cuts were made around the periphery of the retina using dissection scissors. The retina was transferred into 100% glycerol on another slide

using forceps. Vacuum grease was placed around the four corners of the slide and a coverslip carefully added to slowly flatten the retina. Slides were sealed with nail polish.

2.2.4 Immunohistochemistry

An anti-Arrestin3a primary antibody was used (zpr-1; Zebrafish International Resource Center, Cat. No. zpr-1, RRID:AB_10013803) to label double cones (red/green cones) at a 1/100 dilution (see Table 2). The primary antibody was mixed with 2% normal goat serum in PBSTw + 1% DMSO.

The secondary antibody used was AlexaFluor anti-mouse-647 (Invitrogen, Cat. No. A31571, Eugene, OR) at a 1/1000 dilution, also prepared in 2% normal goat serum in PBSTw + 1% DMSO. The retinal tissue was washed for 5 minutes in distilled water, washed for 7 minutes in -20°C acetone, and rinsed in PBSTw + 1% DMSO. The primary antibody was applied and the tissue incubated with the antibody overnight at 4°C. The primary antibody was removed, then the tissue washed with PBSTw + 1% DMSO for 15 minutes, three times. The secondary antibody was applied and incubated overnight at 4°C, in the dark. The secondary antibody was removed, rinsed with PBSTw + 1% DMSO, and the tissue washed with PBSTw + 1% DMSO for 30 minutes. The tissue was allowed to equilibrate in 50% glycerol/PBS. Then 50% glycerol/PBS was then removed, and fresh added, before the retinas were mounted as described above.

2.2.5 Antibody characterization

Zpr-1 was previously determined to recognize Arrestin3a by using zpr-1 to immunopurify its antigen in adult zebrafish retina homogenate [165] (Table 2). Via immunoblotting and immunoprecipitation, it was found that the antigen was a 45kDa protein, and mass spectrometry identified candidate proteins – Arrestin3a (Arr3a) and β-actin. Peptides for the candidate proteins were generated using a protein expression

vector in *E. coli* and immunoblots showed that only Arr3a was immunoreactive with the zpr-1 antibody. There was no reactivity with the negative control (vector only), nor did the antibody detect related arrestins (Arr2a and Arr2b) that were expressed via the *E. coli* protein expression vector. Additionally, when Arr3a was targeted with morpholino knockdown, there was no zpr-1 staining, while there was double cone staining in control embryos.

2.2.6 Ablation of cones

Zebrafish larvae bearing the appropriate nitroreductase transgene were treated with 10mM metronidazole (Sigma-Aldrich, Cat. No. M3761-25G; Oakville, ON) with 0.1% DMSO in E3 media (or just 0.1% DMSO as vehicle-only control), for 1 hour at 7dpf. The larvae were rinsed three times with E3 media, raised in E3 media and euthanized at 9dpf.

2.2.7 Cryosection tissue preparation

To prepare tissue for cryosectioning, tissue was dehydrated in sequential washes: three 20 minute washes of 5% sucrose/0.1M phosphate buffer; a 30 minute wash in 12.5% sucrose/0.1M phosphate buffer; an overnight wash in 20% sucrose/0.1M phosphate buffer; 30 minute wash in a 2:1 ratio of 20% sucrose/phosphate buffer : OCT (VWR, Cat No. 25608-930; Radnor, PA); tissue was then transferred into 1:1 20% sucrose/phosphate buffer : OCT and embedded inside a plastic mold sealed to a glass slide and frozen on dry ice. Tissue blocks were stored at -80°C until cryosectioned. The tissue was cryosectioned at a thickness of 10μm, and applied to Superfrost Plus microscope slides (Fisher Scientific, Cat No. 12-550-15; Ottawa, ON).

2.2.8 Image acquisition and manipulation

Images were obtained on a LSM 700 confocal microscope mounted on a Zeiss Axio Observer.Z1, using ZEN 2010 software (version 6.0, Carl Zeiss AG, Oberkochen). The 63X

or 40X oil objective was used to capture telodendria and the photoreceptor mosaic, and the 20X objective was used for imaging overviews of larval retinas. Images where telodendria are shown were manipulated to increase digital gain, brightness, and contrast in ZEN 2010. Figures were assembled in KeyNote (version 6.6.2, Apple Inc.).

Adobe Photoshop Elements 9 was used to modify select images (Figure 3, bottom row). First, the TIFF images were made black and white (Enhance > Convert black and white). Next, brightness and contrast were adjusted (Enhance > Adjust brightness/contrast > Brightness adjusted to +150, Contrast adjusted to -50). The image was inverted (Filter > Adjustments > Invert) and the background layer duplicated. The new layer had the "Exclusion" layer face applied, producing the final image. For black versus white pixel quantification, these images were inverted (Filter > Adjustments > Invert) so that the background was white and the areas of interest (ie. Cellular structures) were black, then the images were thresholded (Thresholding > +240). Black versus white pixels were calculated in ImageJ.

2.2.9 Metrics

ZEN 2010 software (version 6.0, Carl Zeiss AG, Oberkochen) was used to trace the telodendria and measure telodendria length from pedicle edge to telodendria end; when the telodendria branched, only the longest branch was measured. A telodendria was considered to be an independent process and not a telodendric branch only if there was a single clear origin from the pedicle. Whether the telodendria branched was also recorded. The number of branch points per telodendria was quantified.

To assess the relative spacing/position of pedicles and of cell bodies, we focused on the position of each blue cone pedicle relative to its two neighbouring UV cone pedicles. The distance between the centre of two UV cone pedicles within a row was

determined in Zen software. The centre of the blue cone pedicle that occurred between these UV pedicles was measured relative to the closest UV cone and calculated as a percent distance between the UV cones. Thus a value of 50% represents a blue cone pedicle that was equally spaced between UV pedicles, and lower values indicate the blue cone is closer to one of the UV cones. A similar procedure was carried out for cell bodies.

2.2.10 Statistics

Mann-Whitney U tests were performed in Prism Software (version 7.0 for Mac, GraphPad Software, La Jolla CA). Data is presented as mean ± 1 standard deviation (SD). Each pedicle was treated as an independent unit. The number of pedicles assessed, and the number of fish from which they were imaged, is indicated in the figures. We typically examined three fish per treatment and 20 pedicles per fish, and noted no obvious outliers, which implied this was a representative sample.

2.3 Results

2.3.1 Cone telodendria can be visualized and characterized in adult zebrafish retina

To visualize UV and blue cone photoreceptors, we used confocal microscopy on wholemount adult zebrafish retinas wherein UV and blue cone subtypes were filled with GFP or mCherry proteins, respectively, in *Tg(sws1:GFP;sws2:mCherry)* zebrafish (see Table 1). The cone cell bodies were visualized by imaging optical sections tangentially through the outer nuclear layer (ONL). The cone cell bodies were aligned in the distinct rows known to occur in the adult zebrafish photoreceptor mosaic (Figure 1) [78-80, 119]. We noted that a small percentage of cones were not filled with these fluorescent proteins;

this was due to either lack of transgene expression in some cones or the absence of a cell, though the latter is less likely.

Cone pedicles were visualized by continuing to image in this tangential plane and collecting optical sections at a level immediately apical to the outer plexiform layer (OPL) (Figure 4A). The cone pedicles synapsed with downstream bipolar and horizontal cells, indicated by a hollow centre or "hole" in the pedicle, which is the site of cone pedicle invagination where bipolar and horizontal axons synapse (Figure 4B).

Telodendria extended as fine processes from the pedicles of UV and blue cone photoreceptors (Figure 4A-D). Telodendria were observed to branch off the fluorescently labeled UV and blue cone pedicles in the horizontal plane, in the OPL, located apical (or 'scleral') of horizontal cell nuclei. The telodendria between the UV and blue cones were qualitatively different; the blue cone telodendria appeared to be more numerous and to cover more area. Additionally, UV cone telodendria appeared to often associate with blue cone pedicles within the same row and other UV cones in adjacent rows, while blue cone telodendria appeared to project towards UV cones within the same row, blue cones in adjacent rows, or other (non-visualized) cell types in other mosaic rows (Figure 5).

Retinas were collected during either the daytime (noon-2pm) or nighttime (midnight-2am) to assess whether circadian rhythm influenced the telodendria. In the retinas collected during the day, blue cones typically possessed twice the amount of telodendria per pedicle than UV cones ($p<0.0001$, Mann-Whitney U test; Figure 4E). Similarly, blue cone telodendria branched almost twice as often as UV cone telodendria ($p<0.0001$) (Figure 4F). There was no significant difference between the average length of blue cone and UV cone telodendria (Figure 4G). No significant difference was observed in the number or branching frequency of the UV and blue cone telodendria between the

retinas collected during the day and the retinas collected during the night (Figure 4E,F,H, I).

To represent the coverage of blue cone telodendria and UV cone telodendria in a semi-quantitative manner, images were thresholded and black and white pixels counted (Figure 5). It was found that blue cone telodendria had more than twice the amount of coverage compared to UV cones. However, it should be noted that this number may be slightly exaggerated, as the mCherry channel (used to visualize the blue cones) had slightly more background and some bleed-through of the UV cone pedicles. Nonetheless, the values are a representation of what is apparent – that the telodendria of blue cones cover more area than the UV cone telodendria. This notion is consistent with the observations that blue cone telodendria are more numerous and branch more often (Figure 4).

2.3.2 UV and blue cone pedicles are closely apposed

At the level of the cell body, UV and blue cones appear to be evenly spaced within their rows and not especially associated (Figure 3B). At the pedicle level, the mosaic was still visible, as the blue and UV cones are observed alternating within their well-organized rows (Figure 5, Figure 6). In contrast to the cone cell bodies, the UV and blue cone pedicles were noted to associate unexpectedly within their rows; the pedicles of blue and UV cones are closely apposed in space and often contiguous (Figure 6A-C; Figure 7). This association occurred between UV and blue cones within the same mosaic row, and was consistently polarized (Figure 7). We quantified this by measuring the distance between the centre of a UV cone cell body and the centre of the nearest blue cone cell body, along with the distance between the centre of that original UV cone and the centre of the next UV cone within the same row. The centre of a blue cone cell body was found to

consistently be located about half way between the two UV cone cell bodies (Figure 6D,E). However, when taking similar measurements at the pedicle level (centre of a UV cone pedicle to nearest blue cone pedicle, then from that original UV cone pedicle to the nearest UV cone pedicle), the centre of a blue cone pedicles were distinctly different in their relative position, such that their close apposition leads to their centres being about one third of the way between the centre of UV cone pedicles (Figure 6D,E). Our measures focused on the centres of the cone pedicles to emphasize the spacing, but we also noted the edges of these pedicles were typically (though not always) contiguous and in close contact. This odd spacing of cone pedicles was significantly different ($p<0.0001$, Mann-Whitney U Test) compared to the relative evenly spaced cone cell bodies, demonstrating that the UV and blue cone pedicles typically are more closely associated spatially than would be expected based on the regular spacing of cone cell bodies.

2.3.3 Telodendria can be observed in larval retina throughout development

To determine when in early development UV and blue cone telodendria can first be observed, we looked at retinas from *Tg(sws1:GFP;sws2:nfsb-mCherry*) (Table 1) embryos. As with the adults, retinas were imaged using confocal microscopy taking tangential images from the ONL to the OPL. The larval mosaic is not organized into structured rows like the adult mosaic [78], and this is visible at the pedicle level. We found that telodendria were observable as early as 4 days post fertilization (dpf) (Figure 8A-C).

Telodendria were also visible in 9dpf Tg(*sws1:GFP;sws2:nfsb-mCherry)* larvae retinas (Figure 8D-F). At this developmental stage, the cone pedicles have holes in the centre where downstream cells are innervating into the photoreceptor. In the less mature,

4dpf retina, the cones did not typically have this clear indication of innervation in our imaging approach.

In the control 9dpf larval retina, there are ~25% more telodendria per UV cone pedicle than telodendria per blue cone pedicle (Figure 5H). This is the opposite of what was seen in the adult retina (Figure 4), where we observed more telodendria per blue cone than per UV cone.

2.3.4 UV cone telodendria do not notably change following blue cone ablation

Since we had previously seen rapid recovery of visually-mediated behaviour post blue cone ablation, we investigated whether the other short wavelength sensitive cones, UV cones, were undergoing telodendric alterations in response to blue cone loss [132]. We took advantage of a well characterized line that expresses nitroreductase (NTR; *nfsb* gene) in blue cones, *Tg(sws2:nfsb-mCherry)* [103], and crossed it with a line that expresses GFP in UV cones (*Tg(sws1:GFP)*; Table 1). Targeted cone ablation was accomplished by taking advantage of a zebrafish line expressing NTR in blue cones (Table 1). Nitroreductase converts prodrugs – in this case, metronidazole (MTZ) – into DNA cross-linking agents, inducing apoptosis [119, 131, 132]. The larvae were treated at 7dpf with either MTZ or vehicle control for one hour, the treatment was removed, and the larvae were euthanized at 9dpf.

Following blue cone ablation, the number of telodendria per UV cone was not significantly different than that of the control group (Figure 8I, $p>0.05$). Thus, it does not appear that the number of UV cone telodendria are altered as a result of blue cone loss.

2.3.5 Overabundance of fluorescent protein in cone cells results in degeneration

As there was no statistical difference in the UV cone telodendria number post blue cone loss, we sought to investigate whether remaining cones of the target cell type were undergoing telodendric plasticity after partial ablation of the cone subtype population. To do this, we utilized zebrafish lines wherein only ~80% of the target cone type is ablated (*Tg(sws1:KalTA4;UAS:nfsb-mCherry-KalTA4)* and *Tg(sws2:KalTA4;UAS:nfsb-mCherry-KalTA4)* to ablate UV and blue cones, respectively) [132]. These lines were crossed with fish that expressed GFP in the cone type of interest (either *Tg(sws1:GFP)* or *Tg(sws2:GFP)*) to produce *Tg(sws1:KalTA4;UAS:nfsb-mCherry-KalTA4;sws1:GFP)* and *Tg(sws2:KalTA4;UAS:nfsb-mCherry-KalTA4;sws2:GFP*) fish. As these fish would then have GFP expressed in the remaining non-NTR expressing cones of the target type, these cones could be investigated for telodendric alterations. However, while each line independently had healthy fluorescently labeled photoreceptors, we observed cone degeneration in the combination fish (Figure 9). The retinas were missing cells, and many of the remaining fluorescently labeled cones were dysmorphic in appearance. Additionally, the surviving cones often appeared to express only one fluorescent protein, either mCherry or GFP; this could be because expressing both resulted in cell death, and there was some selection to express only one fluorescent marker or the other. To conclude, it appears that overexpression of fluorescent protein within UV or blue cones leads to degeneration, similar to what has been seen in a zebrafish model of rod degeneration, wherein rods overexpress CFP and subsequently die [140].

2.3.6 *Rod telodendria are less numerous than short wavelength cone telodendria in larvae*

Characterization of photoreceptor telodendria has historically focused primarily on cones rather than rods. To investigate rod telodendria in zebrafish larvae, we crossed *Tg(rho:GFP)* fish, which express GFP in their rods, with *Tg(sws2:nfsb-mCherry)* fish. These fish were grown to 9dpf and *Tg(rho:GFP;sws2:nfsb-mCherry)* retinas were dissected and imaged. Rod spherules are located more basally than the cone pedicles (Figure 10A), and thus the rod and cone synaptic terminals are often captured in slightly different visual planes (Figure 10B-D). Rod photoreceptor telodendria are visible, and at this age, the rods appear to still be somewhat immature, with wide spherules that have not yet become tapered above the synaptic terminal (Figure 10C). The rod telodendria appear to connect to typically converge on other rods, or to reach to other cells within the photoreceptor layer. Rods in the larval retina have fewer telodendria than was observed in the UV ($p<0.0001$) and blue cones ($p<0.0001$) (Figure 10E). In conclusion, it appears that rods are making fewer connections than the short wavelength cones and connect with rods or other cells.

2.3.7 *UV cone telodendria in lots-of-rods mutants are reduced in number*

To assess if UV cone telodendria would be affected when UV cones are in low density, we assessed *tbx2b* mutant fish. The *tbx2b*^{lor} (herein referred to as "*lor*") mutant retina possesses an atypically high abundance of rods, and few UV cone photoreceptors [166, 167] (Figure 11A-B; Table 1). UV cone telodendria were imaged in larval retinas of 9dpf *lor*;*Tg(sws1:GFP)* fish. UV cone telodendria were observed to be present, but were noticeably more tortuous and randomly oriented than wild-type larval UV cone

telodendria (Figure 8C). The average number of telodendria per UV cone pedicle in the *lor* retina was reduced by half compared to the number of UV cone telodendria in Tg(*sws1:GFP;sws2:nfsb-mCherry*) retinas (Figure 8H, 11D); this is significantly different ($p<0.0001$).

2.4 Discussion

Telodendria are conserved structures that may play important roles in shaping the synaptic outputs of vertebrate photoreceptors, yet little is known about their morphology and function. Here, we characterized telodendria in adult and larval zebrafish by utilizing fluorescent markers expressed in UV and blue cones. We found that in the adult retina, blue cones have more telodendria than UV cones, and blue cone telodendria branch more frequently than UV cone telodendria – this did not differ between the day and night. Blue cones thus appear to be making more connections with other photoreceptors than UV cones are. This differs from what has been observed in other fishes. The walleye retina consists of green and orange-sensitive cones [168] which send telodendria out to one another [154]. Telodendria in the walleye retina are less numerous than what we observed in zebrafish, with walleye cones typically projecting 5 telodendria per pedicle, regardless of subtype [154]. The average length of walleye cone telodendria was thrice that of zebrafish telodendria [154]; this could be due to the spectral subtype of cone investigated being different, or represent a general connectivity difference due to photoreceptor mosaic structure and cone subtype density or abundance. In the future, zebrafish red and green cone telodendria could be characterized and connectivity compared to that of other fishes.

No morphological alterations were detected in the telodendria between the retinas collected during the day versus night, suggesting that circadian rhythm is not inducing

physical changes at these time points. It is known that the retina responds to circadian rhythm, and that photoreceptor electrical coupling can be different depending on circadian clock [169]. Likely there are changes at the gap junction level that impact how the photoreceptors communicate with one another between the day and night, while the cellular morphology is relatively stable.

Contrary to what we observed in adult zebrafish in relation to UV and blue cone telodendria abundance, larval UV cones possess more telodendria than larval blue cone telodendria. This differing connectivity between adult and larval cones could potentially relate to the disparate organization of the photoreceptor mosaic between these two life stages. In the adult retina, the cones form a predictable row mosaic, with blue and UV cones existing in a 1:1 ratio [78]. The larval cone mosaic is not as well formed, and cone ratios are not the same as that of the adult retina [78] – thus, the number of telodendric connections could be altered at this life stage due to differential potency of pathfinding queues and/or different proximal cell types. Alternatively, there could be developmental milestones that have not been reached that lead to a change in telodendria connectivity, such as increased activity of specific cone types or pruning of abhorrent connections. Other synaptic elements of zebrafish cone pedicles are known to mature over this developmental window, including the number of ribbons and spinules increasing in the cone pedicles [170, 171].

Cone telodendria connectivity patterns vary widely between species, likely due to photoreceptor mosaic organization and cone type abundance. Indeed, telodendria have been investigated in several turtle species, and these species typically exhibit differing telodendric patterns. Blue cones in the turtle species *Geoclemys reevesii* make telodendric connections with red and green cones, but not other blue cones, while red cones make connections with both red and green cones, and green cones connect with

blue and red cones [85]. In *Chelydra serpentina* and *Pseudemus scripta elegans*, red cones and green cones connect to one another indiscriminately [111, 146]. In adult zebrafish, blue cone telodendria appear to generally connect with other blue cones or non-visualized photoreceptors in the immediately adjacent rows, while UV cone telodendria appear to typically project to neighbouring blue cones or across to UV cones in adjacent rows. In the future, we could determine which photoreceptor subtypes blue cones are contacting and compare this to what has been seen in other species where telodendria have been investigated in similar detail.

In the human retina, blue cones (*sws1* cones, homologue of zebrafish UV cones) do not typically send out telodendria, but are contacted by nearby green and red cones, as well as rods [96, 159, 172, 173]. Similarly, in macaque retina, blue cones were found to have few, if any, short processes that did not connect to other cones [144, 161] while green and red cones had telodendria that connected to all cone types [144]. This is very different from zebrafish UV cones (*sws1* cones), which have robust telodendric processes that connect with other short wavelength cones, and what has been seen in other animals that have had telodendria investigated. The absence of *sws1* cone telodendria seems to be an intriguingly unique feature of primate blue cones. Why these cones do not form extensive telodendric connections like what is seen in other primate cones or the *sws1* cones of other vertebrate species is unknown. Understanding how *sws1* cones integrate and behave in other vertebrates can provide insights into what causes primate blue cones to be so peculiar. The genetically tractable zebrafish system can continue to be investigated for factors that influence telodendric growth, and how changes in photoreceptor abundances influences telodendria.

Here, we found that zebrafish mutants with retinas containing an abnormally high abundance of rods and few UV cones have fewer telodendria than wild-type larvae. This

reduction in telodendria could be the consequence of fewer UV cones; the development of the UV cone connectivity pattern could be dependent on communication or secreted factors by other UV cones, and thus the absence of a typical proportion of cones results in fewer connections. Alternatively, the excess number of rods could be inhibiting UV cone telodendric development. In the future, factors involved in telodendric pathfinding could be investigated. Potential factors involved in this pathfinding are protocadherins, which are associated with self-recognition during axon and dendritic pathfinding [174-176]. Semaphorin3A is a factor known to promote dendrite formation and suppress axon growth [177] – this factor could be involved in telodendria formation as well. Regardless, our data do not support the notion that absence of UV cone neighbours leads to the remaining UV cones having more elaborate telodendria to fill their respective fields.

We did not note any alterations in UV cone telodendria number after targeted ablation of blue cones in larval zebrafish. However, this does not necessarily mean that UV cone telodendria do not undergo changes after blue cone loss – rather, we may have missed the window where changes are occurring, or the changes occur outside the simple morphology we quantified. In the future, we could assess more time points, assess gap junction properties, and determine whether the UV cone telodendria are making contacts with different cone types after blue cone death, which could be part of the underlying mechanism behind rapid recovery of visually mediated behaviour post blue cone ablation [132]. For instance, UV cone telodendrites that may usually connect with blue cones may re-route to a different photoreceptor type after blue cone death.

The unexpected spatial coupling observed between UV and blue cone pedicles likely has a functional consequence, and zebrafish UV and blue cones may communicate with one another more than was previously thought. The contiguous apposition of these pedicles contrasts the even spacing of their cell bodies, and is reminiscent of the close

intertwining of individual cones into double cones in most non-amniotic vertebrates. The members of double cones are coupled by gap junctions [178-181], though our conjecture should be tempered by the admission that the function of double cones, and how any such coupling allows differentially signal processing compared to single cones, is largely unknown. The nature of this association, and whether there is synaptic communication between the UV and blue cone pedicles at the sites where there is direct contact is also not known. Both being short wavelength sensitive cones, the pairing of the pedicles may allow for communication between the UV and blue cones to increase sensitivity. Blue cones that are without a UV cone neighbour, such as in *tbx2b* mutants, could be assessed morphologically and using electrophysiology to determine whether the unpaired blue cones behave in a different manner than blue cones with a UV cone partner.

Historically, telodendria characterization has been focused on cone photoreceptors and not rods. This focus on cones may be due to interest in high acuity and colour vision processing, the cone-rich non-mammalian models that were utilized for early telodendric characterization, and known identity of the cone connexin. We found that in the larval retina, rods have fewer telodendria per synaptic terminal than the short wavelength cones, and these telodendria appear to connect to either rods or other cells in the photoreceptor layer. How this changes between the larval and adult zebrafish life stages could be investigated in the future, as well as what photoreceptor subtypes the rods are specifically interacting with, and how the telodendria frequency and connectivity partners compare to that of other diurnal or nocturnal species.

Vision can only be accomplished if the appropriate connections are generated and maintained with the required cell types within the visual system. Knowledge of telodendria can aid in determining whether photoreceptors are successfully integrating into the neural retina during development and regeneration. Introduction of

photoreceptor precursors into host retina has resulted in a wide range of reported integration success rates [55, 61-63, 182, 183], but whether these introduced cells are truly forming stable connections with the necessary cell types has been difficult to determine. Deciphering the connectivity patterns of telodendria and how these connections are re-established after regeneration is essential for the accurate assessment of stem cell therapies, which rely on donor photoreceptors appropriately integrating into the retina and becoming functional. Telodendria provide a morphological determinant of integration into the photoreceptor layer; if the donor photoreceptors are forming telodendric connections, then they are likely communicating with surrounding cells and may be becoming functional. Learning how telodendria form connections and how they are involved in cellular communication is essential for complete understanding of the retinal connectome and how vision is achieved.

Table 1. Genotype and description of the zebrafish lines used.

Genotype	Description	ZFin ID	Reference
Tg(sws2:mCherry)^{ua3011}	The blue opsin promoter drives the expression of mCherry in blue cones.	ZDB-ALT-130819-1	[115]
Tg(sws1:GFP)^{kj9}	GFP is expressed in UV cones from the UV opsin promoter.	ZDB-ALT-080227-1	[184]
Tg(sws2:nfsb-mCherry)	This line expresses a nitroreductase(*nfsb* gene)-mCherry fusion protein in blue cones (sws2). Nitroreductase is a reducing agent that converts otherwise inert prodrugs (such as metronidazole) into DNA cross-linking agents, inducing targeted ablation. The mCherry tag allows visualization of these cells.	Not available	[103, 185]
Tg(rho:eGFP)^{kj2}	GFP is expressed in rods via the rhodopsin promoter.		[186]
"UV kaloop" *Tg(sws1:KalTA4; UAS:nfsb-mCherry-KalTA4)*$^{ua3137;ua3139}$	Expression of nitroreductase-mCherry fusion protein in UV cones via KalTA4-UAS system. *Sws1* drives the expression of KalTA4, a transcription factor that recognizes the UAS promoter; this leads to expression of nfsb-mCherry,		[132]

	as well as the production of more KalTA4, creating a positive feedback loop. ~80% of UV cones express the nitroreductase-mCherry protein. UAS is frequently inactivated in adult zebrafish.		
"Blue kaloop" *Tg(sws2:KalTA4; UAS:nfsb-mCherry-KalTA4)*$^{ua3135;ua3136}$	Expression of nitroreductase-mCherry fusion protein in blue cones via KalTA4-UAS system. See above. ~80% of blue cones express.		[132]
tbx2b^{lor}	"lots-of-rods" mutants; this line is characterized by having an atypical abundance of rods, but few UV cones	ZDB-ALT-080920-1	[166]

Table 2. Antibodies used, including antigen recognized by the antibody, immunogen used to generate the antibody, source, catalogue number, species raised in, and concentration.

Antibody	**Antigen, structure of immunogen that the animal was immunized**	**Manufacturer, Cat. No., RRID, species, mono/polyclonal**	**Dilution**
Zpr-1	Arrestin3a Whole zebrafish retinal cells	ZIRC Cat. No. Zpr-1 AB_10013803 Mouse Monoclonal ZFin ID: ZDB-ATB-081002-43	1:100

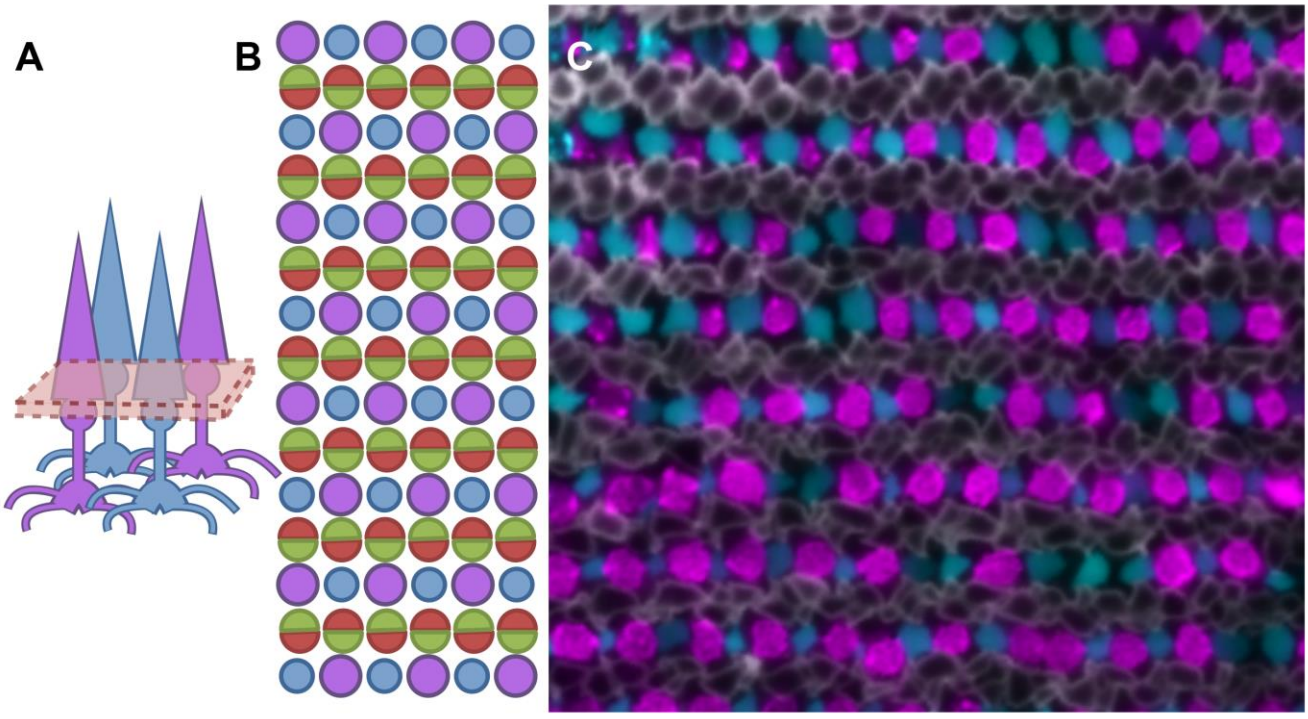
A
B
C

Figure 3. Cone photoreceptors of zebrafish are patterned into a mosaic.

(A) Schematic of UV and blue cone photoreceptors indicating a plane of optical section at the level of cone cell bodies. **(B)** A cartoon of the zebrafish cone photoreceptor mosaic at the level of cone cell bodies in the plane of section indicated by the dotted lines in panel A (i.e. in the 'tangential' plane, orthogonal to the photoreceptor long axis), with UV, blue, green and red cones depicted in their cognate colours. Red and green cones are fused into double cones and form rows. These rows of double cones are positioned between rows of alternating UV and blue single cones. **(C)** The zebrafish adult cone mosaic imaged in transgenic zebrafish expressing GFP in UV cones, and expressing mCherry in blue cones (*Tg(sws1:GFP; sws2:mCherry)*; blue cones are pseudo-coloured blue, and UV cones are pseudo-coloured magenta). Micrograph is a confocal optical section through the cone cell bodies. Double cones (both red and green cones) are labelled with an antibody against arrestin3a, depicted in grey. Rare gaps in the pattern of alternating UV and blue cones are assumed to typically represent incomplete penetrance of transgene expression, though in some instances could also represent the absence of a cone.

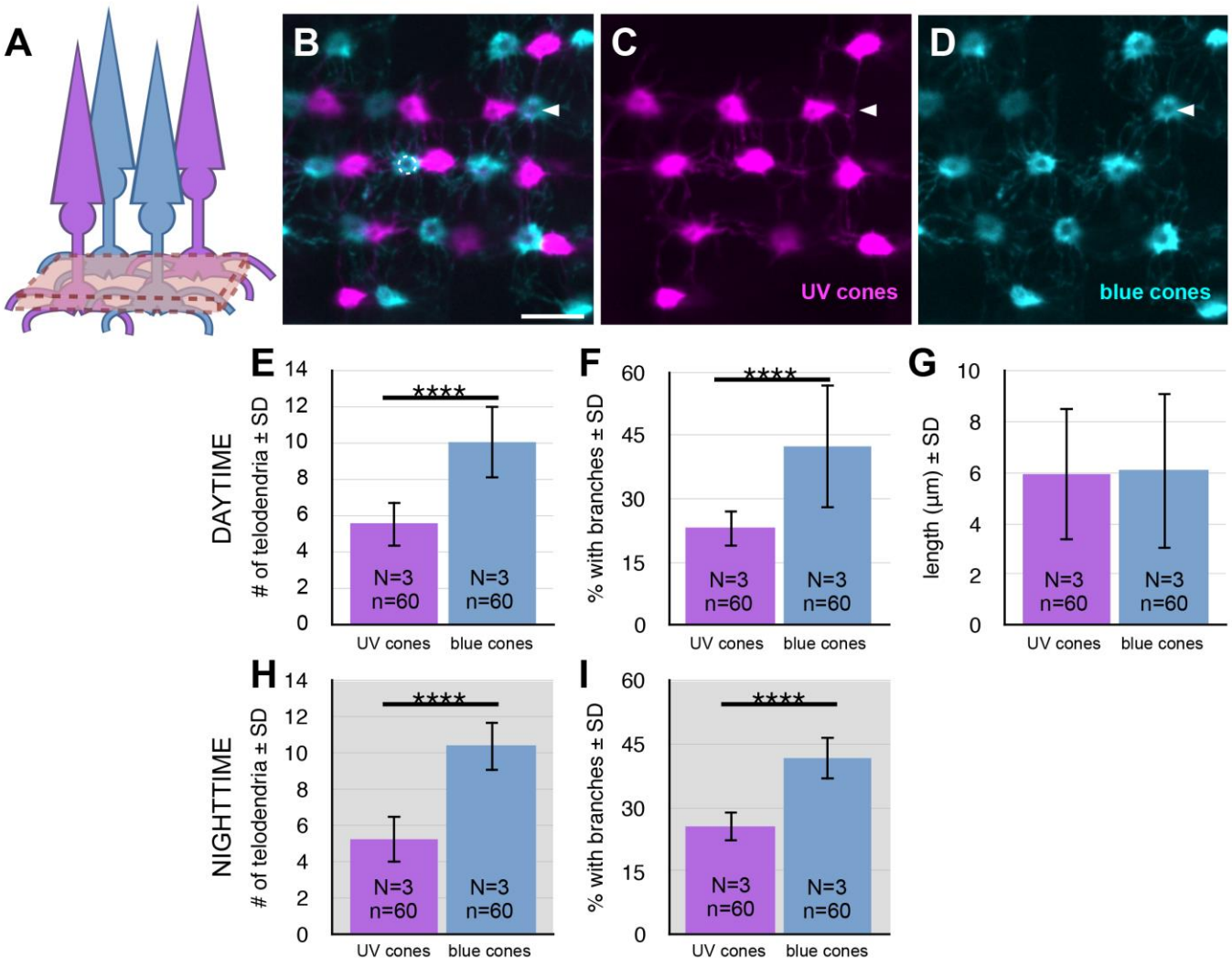
A
B
C
UV cones
D
blue cones
E
DAYTIME
# of telodendria ± SD
****
N=3
n=60
N=3
n=60
UV cones
blue cones
F
% with branches ± SD
****
G
length (µm) ± SD
H
NIGHTTIME
I

Figure 4. Telodendria can be visualized in adult zebrafish retina via fluorescent markers expressed within the cones and the telodendria do not detectably change in response to circadian rhythm.

(A) A schematic of UV and blue cone photoreceptors depicting the plane of optical section through the cone pedicles. **(B)** Telodendria, fine processes extending in the tangential plane between cone pedicles, are detectable and amenable to study in the retina of Tg(sws1:gfp;sws2:mCherry) zebrafish, which express GFP in UV cones (via the sws1 promoter), and express mCherry in blue cones (via the sws2 promoter). Blue cones are pseudo-coloured blue, and UV cones are pseudo-coloured magenta. In the centre of the pedicles, a hole can be seen (indicated by dashed circle) — this is where downstream cells are making contact with the cone photoreceptors. Arrowhead denotes UV cone telodendria that appear to be converging on a blue cone pedicle. **(C)** UV cone pedicles and telodendria; and **(D)** blue cone pedicles and telodendria**. (E)** The average number of telodendria per UV and blue cones, ± standard deviation (SD). In adult retinas collected during the day, UV cones have half as many telodendria than blue cones. **(F)** The percentage of blue and UV cone telodendria with branches. Blue cone telodendria are branched twice as often than UV cone telodendria. **(G)** The average length (μm) of the UV and blue cone telodendria is not significantly different. **(H)** Number of UV cone and blue cone telodendria in retinas that were dissected out during the night. The number of telodendria was not significantly different from that of the daytime retinas. **(I)** The percentage of UV and blue cone telodendria that branch in retinas dissected out during the night. The branching of the telodendria was not statistically different from the telodendria in the retina dissected during the day. N=3 retinas, 20 pedicles were counted per retina. ****=$p<0.0001$, Mann Whitney U tests. Scale bar = 10μm.

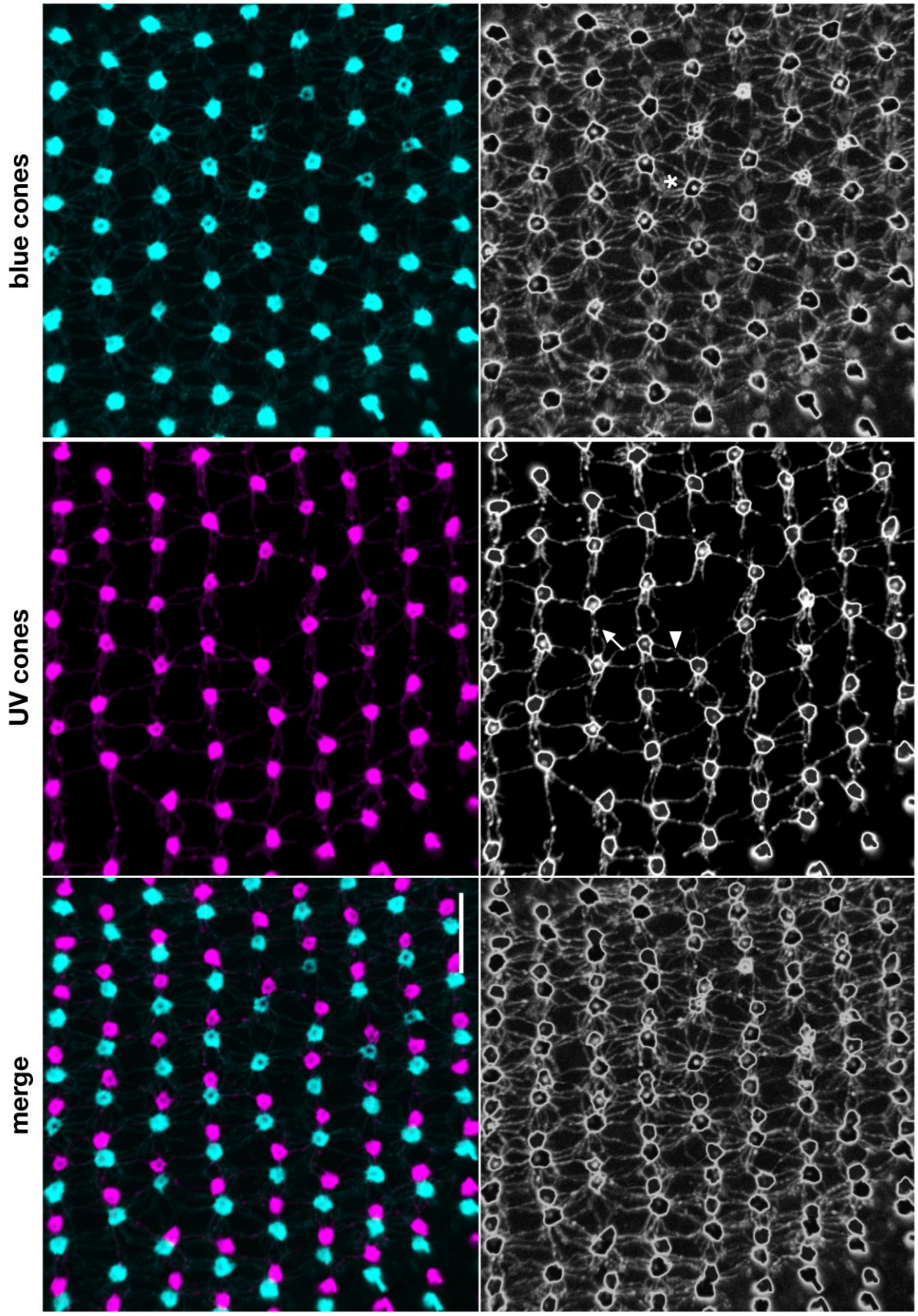
blue cones
UV cones
merge

Figure 5. Blue cone telodendria cover more area than UV cone telodendria.

Top panels: confocal images of adult *Tg(sws1:GFP;sws2:mCherry)* retinas, wherein UV cones are labelled with GFP and blue cones with mCherry. Telodendria can be seen sprouting from the pedicles. UV cones are pseudo-coloured magenta, while blue cones are pseudo-coloured cyan. Bottom panels: Manipulation of images (top panels) to make the UV and blue cone telodendria patterning more visually apparent. The UV and blue cone telodendria are visibly different in coverage and connectivity. The UV cone telodendria often travel within their own row, appearing to contact neighbouring blue cones (arrow), or between rows, appearing to contact other UV cones (arrowhead). In contrast, blue cone telodendria project in all directions. Blue cone telodendria appear to converge on UV cones within the same row, blue cones in adjacent rows, as well as on non-visualized cells in other rows, such as double cones or rods (asterisk). After thresholding and colour inversion, the numbers of black and white pixels were obtained, and the black pixels (telodendria) were divided by the total number of pixels. The UV cone telodendria produced a value of 0.21 pixels/area and the blue cone telodendria produced a value of 0.53 pixels/area. This demonstrates the additional area coverage by blue cone telodendria compared to UV cone telodendria. Scale bar = 20μm.

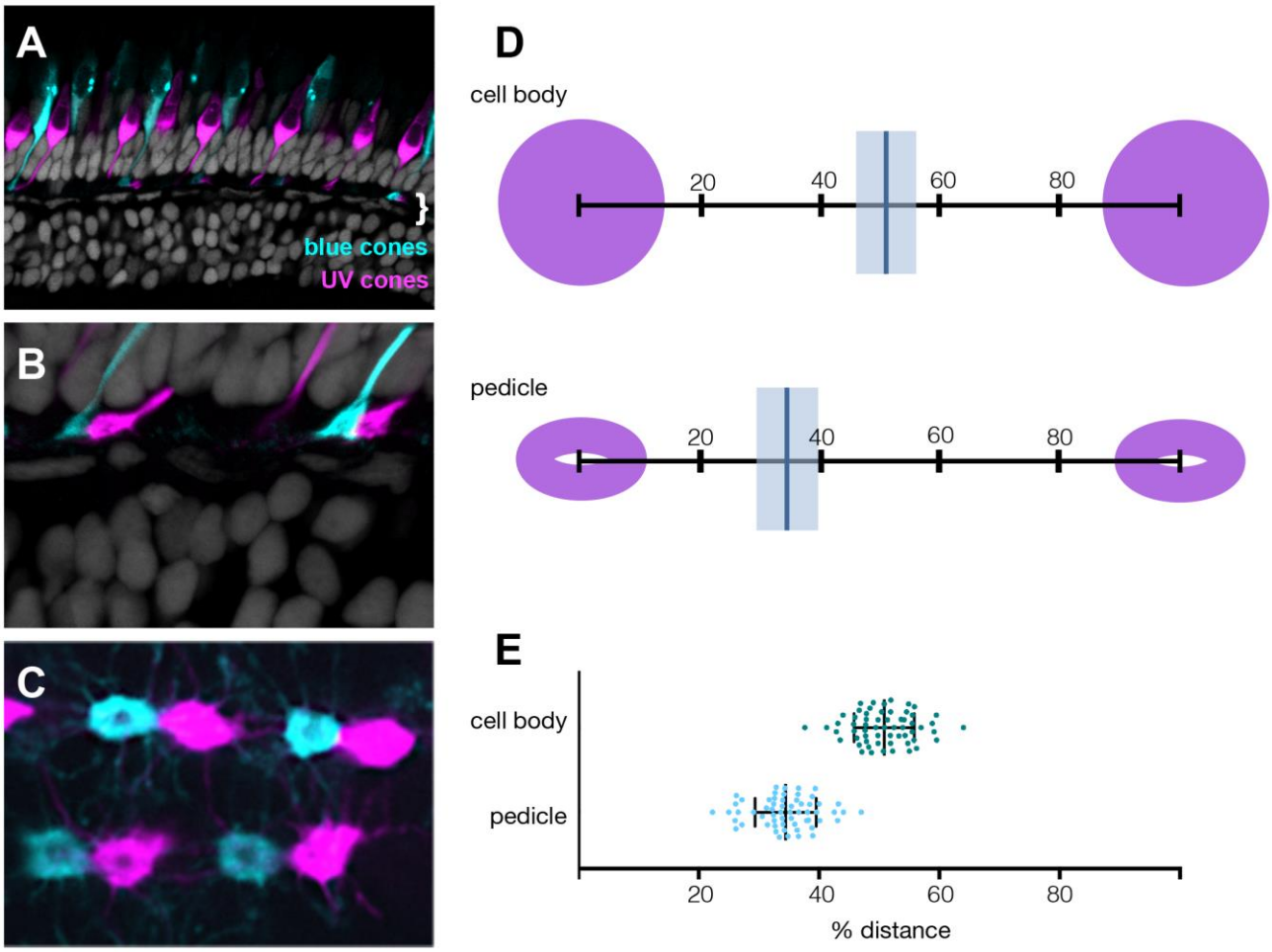
A
blue cones
UV cones
B
C
D
cell body
20
40
60
80
pedicle
20
40
60
80
E
cell body
pedicle
20
40
60
80
% distance

Figure 6. Pedicles of UV and blue cones are paired.

(A) Transverse sections of *Tg(sws1:gfp;sws2:mCherry)* zebrafish retina, with UV cones (*sws1*) labeled with GFP and blue cones (*sws2*) labeled with mCherry. UV cones are pseudo-coloured magenta and blue cones are pseudo-coloured cyan. Nuclei are in grey. **(B)** Increased magnification, focusing on the outer plexiform layer depicted by the white bracket in (A). The association between UV and blue cone pedicles, where one UV cone pedicle is paired with a blue cone pedicle, is visible. **(C)** Confocal image of cone pedicles in whole mount retina, again showing the association between the UV and blue cone pedicles. **(D)** The typical position of a blue cone, expressed in percentage distance between the two closest UV cone cell bodies. While the centre of blue cone cell bodies are found about half of the way between UV cone cell bodies (i.e. equidistant from both UV cone cell bodies, top schematic – vertical line = 50% ± standard deviation indicated by shading), the centre of the blue cone pedicle is found about a third of the way between UV cone pedicles, which is closer than would be expected (bottom schematic). **(E)** Scatter plot of the raw values of percentage distance between UV cone bodies or pedicles, as depicted in (D). The values are closely clustered, demonstrating that the centres of the blue cone cell bodies tend to lie halfway between the UV cone cell bodies (teal scatterplot), whereas the centres of the blue cone pedicles tend to lie closer to one UV cone pedicle than the other (blue scatter plot). N=3, 20 pedicles/retina.

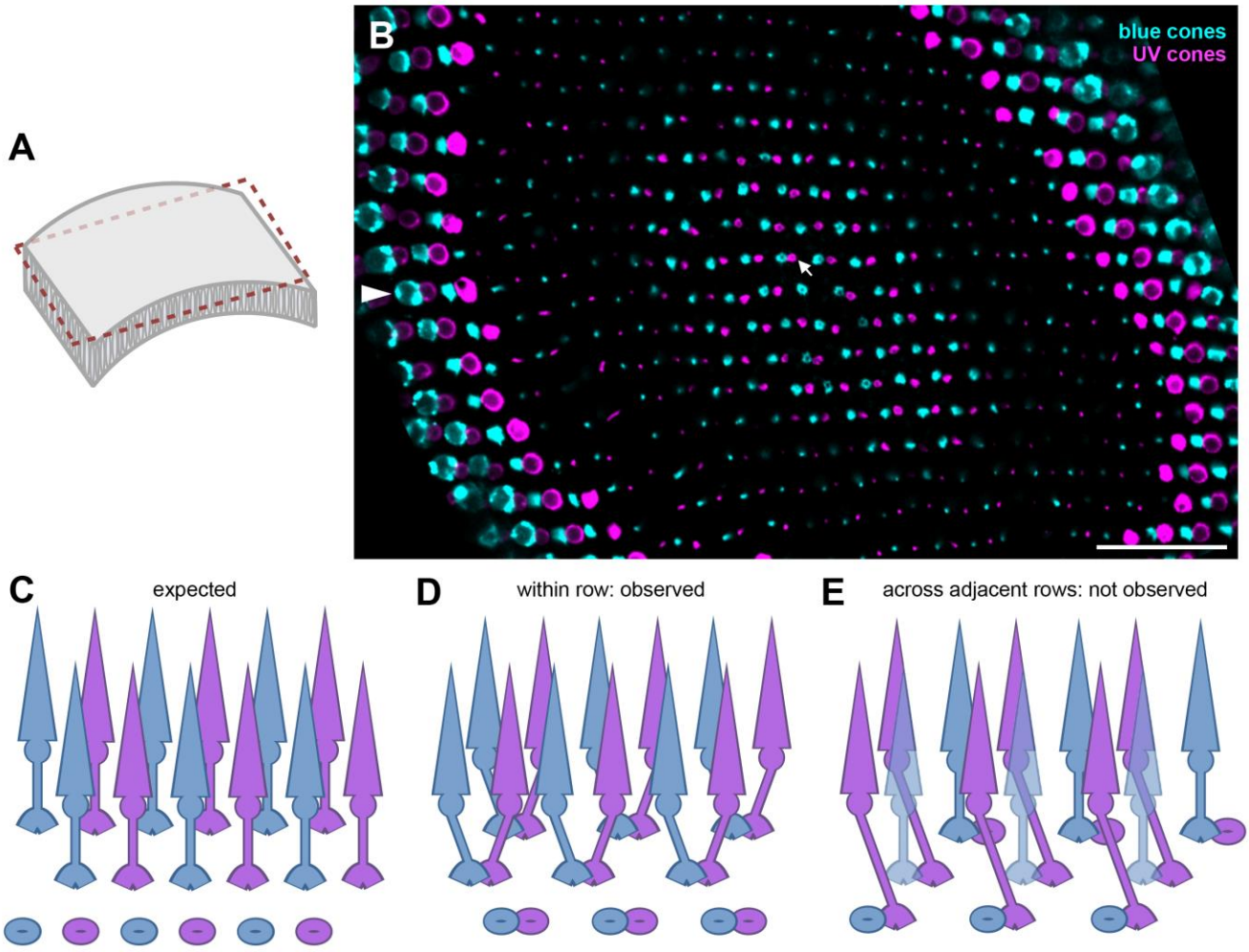
A
B
blue cones
UV cones
C
expected
D
within row: observed
E
across adjacent rows: not observed

Figure 7. Organization of the UV and blue cone cell bodies and pedicles within the row mosaic.

(A) Depiction of how the retina was sectioned to produce what is observed in (B). As the retina is rounded, it was possible to obtain a section that cuts through slightly different regions within the retina, allowing for visualization of different cellular components. **(B)** *Tg(sws1:GFP; sws2:mCherry)* retina that was sectioned such that UV and blue cone the cell bodies are visible on the periphery and the pedicles are seen in centre. Within a row (arrowhead) the cell bodies appear evenly spaced, and the row can be followed down to the pedicle. At the pedicle, UV and blue cones are paired (arrow). Regardless of the level being investigated, the cone elements are always in a row, and there is no apparent twisting or crossing over of the cells into neighbouring rows. This indicates that the pedicle association is occurring between UV and blue cones within the same row. In the centre of the pedicles is a visible hole, where the downstream neurons are innervating with the cones. GFP is pseudo-coloured magenta and mCherry is pseudo-coloured cyan. Scale bar = 50μm. **(C)** The expected organization of the UV and blue cone cell bodies and pedicles. The short wavelength cone cell bodies and pedicles are evenly spaced within their rows. **(D)** Cartoon of UV and blue cone cell body and pedicle organization that was actually observed. The photoreceptor cell bodies are evenly spaced within rows, and the pedicles associate between pairs of UV and blue cones within the same row. **(E)** A potential organization of the cone cell bodies and pedicles, where the cone pedicles reach out of the row the cell body is located in and twists into the adjacent row to allow pedicle association. The blue cones in the middle row are translucent to emphasize the twisting of the UV cone in the row behind, such that the cell body is in the far row but the pedicle is in the next (middle) row. This was not observed.

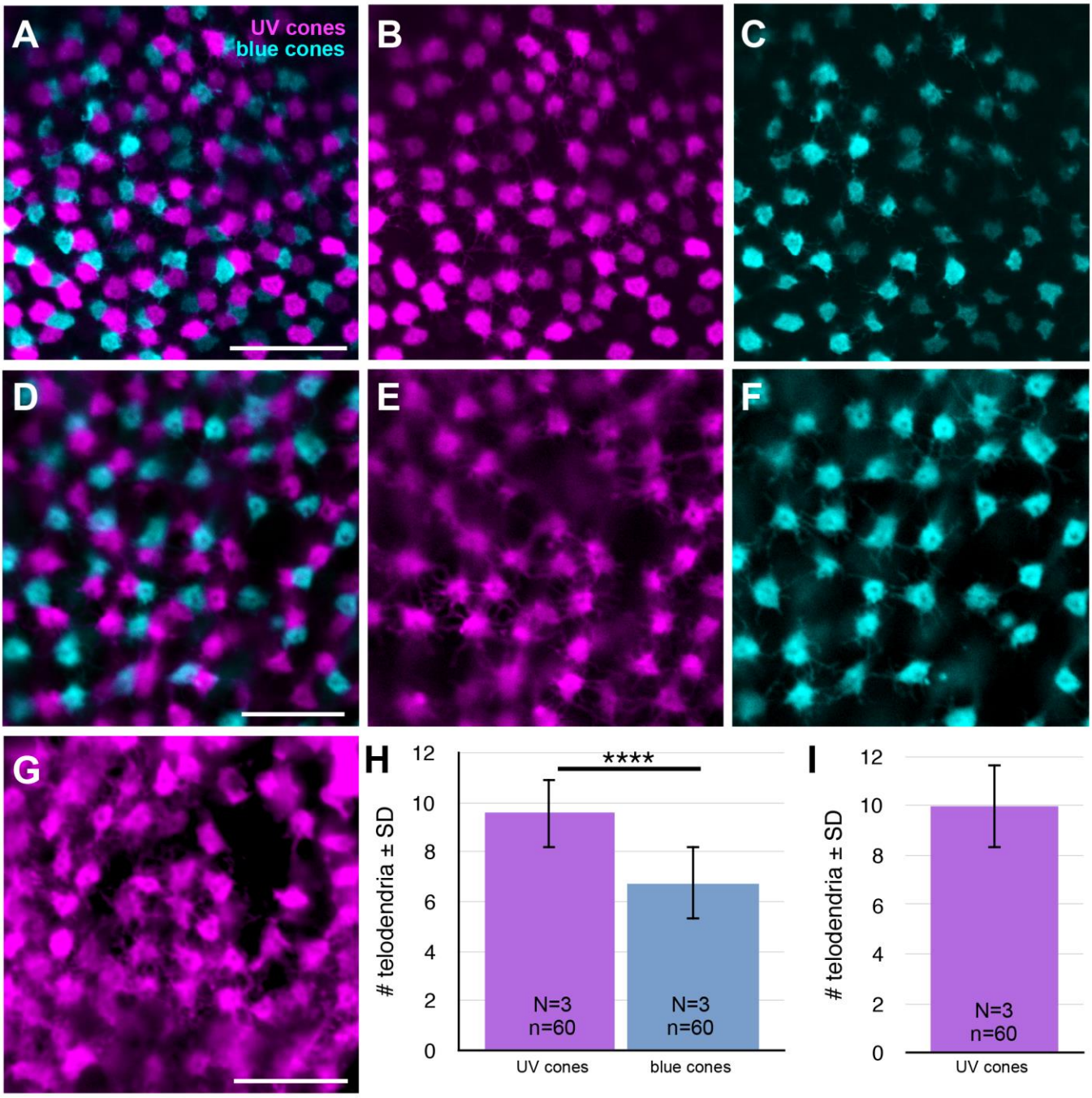
A
UV cones
blue cones
B
C
D
E
F
G
H
telodendria ± SD
12
10
8
6
4
2
0
****
N=3
n=60
N=3
n=60
UV cones
blue cones
I
telodendria ± SD
12
10
8
6
4
2
0
N=3
n=60
UV cones

Figure 8. Telodendria can be seen early in development and number of larval UV cone telodendria does not change in response to blue cone ablation.

(A-C) Telodendria in 4 days post fertilization (dpf) *Tg(sws1:GFP; sws2:nfsB-mCherry)* retina, wherein GFP is expressed in UV cones (*sws1* promoter) and a nitroreductase (NTR)-mCherry fusion protein (*nfsB-mCherry*) is expressed in blue cones (*sws2*). The mCherry allows for visualization of the photoreceptors expressing the transgene, while nitroreductase is a reducing agent that allows for the targeted ablation of cells when exposed to otherwise harmless prodrugs (such as metronidazole, MTZ). Note the less organized mosaic in the larval retina, compared to the adult retina. Scale bar = 10μm. **(D-F)** Telodendria in 9dpf *Tg(sws1:GFP; sws2:nfsB-mCherry*) zebrafish larval retina, which were used for quantification of telodendria number. Similar to the adult cone pedicles, the larval cone pedicles have an invagination in the centre, where downstream neurons are contacting them, and are generally closely associated. **(G)** Pedicles and telodendria in 9dpf *Tg(sws1:GFP; sws2:nfsb-mCherry)* treated with MTZ to ablate blue cones. Note the absence of UV cones. **(H)** Number of UV and blue cone telodendria in control larval retinas; there are more telodendria per UV cone pedicle than telodendria per blue cone pedicle. **(I)** Larvae were exposed to MTZ at 7dpf to induce blue cone ablation, then fixed at 9dpf for visualization. The number of UV cone telodendria post blue cone ablation was not significantly different from the number of UV cones in the non-ablated zebrafish in (G). Scale bars = 10μm.

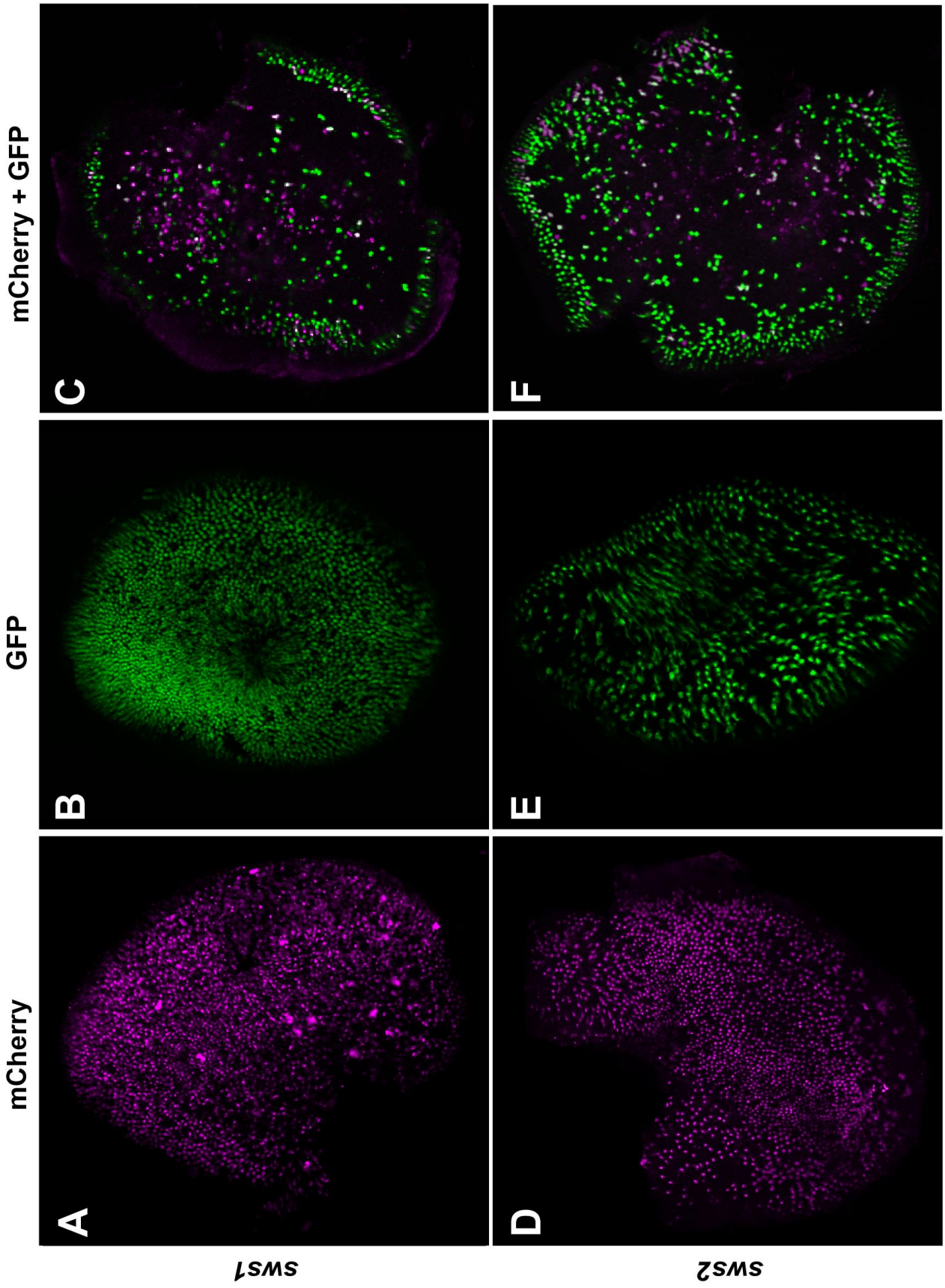
mCherry
GFP
mCherry + GFP
A
B
C
D
E
F
SWS1
SWS2

Figure 9. Excess fluorescent protein within photoreceptor cells leads to degeneration.

Retinas dissected from 9dpf larval zebrafish expressing fluorescent protein in either UV (*sws1*) or blue (*sws2*) cones. **(A)** Retinas from *Tg(sws1:KalTA4;UAS:nfsb-mCherry-KalTA4)* and **(D)** *Tg(sws2:KalTA4;UAS:nfsb-mCherry-KalTA4)*) with mCherry pseudo-coloured magenta. These lines express the nitroreductase-mCherry (NTR-mCh) fusion protein under the control of the KalTA4-UAS system. In either blue or UV cones, the KalTA4 transcription factor is expressed, and KalTA4 recognizes the UAS promoter to drive expression of NTR-mCh. Behind the NTR-mCh in the transgene is more KalTA4, which generates a positive feedback loop. **(B)** *Tg(sws1:GFP)* larvae retina, where GFP is expressed in UV cones, and **(E)** *Tg(sws2:GFP)* larval retina, where GFP is expressed in blue cones. GFP is pseudo-coloured green. **(C)** A retina from a *Tg(sws1:KalTA4;UAS:nfsb-mCherry-KalTA4;sws1:GFP)* larvae. **(F)** Dissected retina from a *Tg(sws2:KalTA4;UAS:nfsb-mCherry-KalTA4;sws2:GFP)* larvae. In (C) and (F) the photoreceptors are absent from large portions of the retina, and the remaining cells appear dysmorphic. Many of the remaining cones have only one fluorescent protein expressed. It appears that the amount of fluorescent proteins expressed in the cells is resulting in their degeneration.

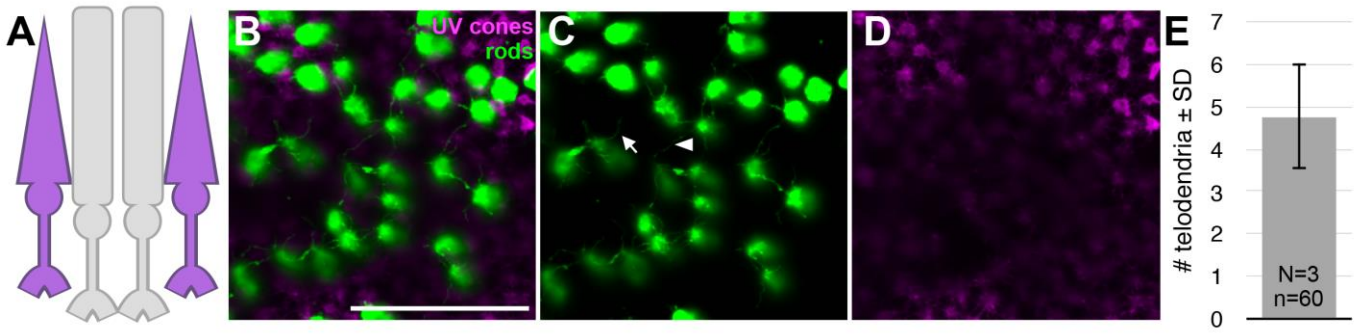

Figure 10. Rods have fewer telodendria than the short wavelength cones.

(A) Cartoon depiction of UV cone and rods. The rod spherules are located more basally than the cone pedicles. **(B-D)** Retina from a *Tg(sws1:nfsb-mCherry; rho:GFP)* 9dpf larvae, wherein GFP is expressed within UV cones and NTR-mCherry is expressed in UV cones. GFP is pseudo-coloured green, and mCherry is pseudo-coloured magenta. UV cone telodendria are visible from the UV cone pedicles, and rod telodendria are visible from the rod spherules. The rod telodendria appear to often converge on other rods (arrowhead) or to reach for other cell types (arrow). **(E)** Rods tend to have fewer telodendria than what was observed in the blue ($p<0.0001$) and UV cones ($p<0.0001$) (N=3, 20 pedicles counted/retina). Scale bar = 20 μm.

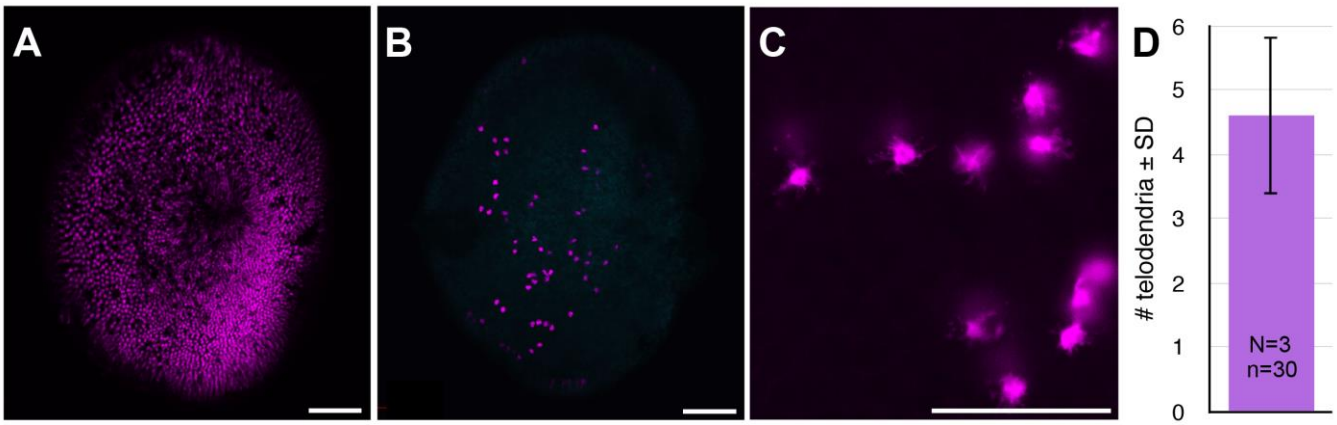

Figure 11. UV cone telodendria are reduced in *lor* mutant retinas.

(A) Wild-type 9dpf *Tg(sws1:GFP)* retina, where GFP is expressed in UV cones and **(B)** 9dpf homozygous *lots-of-rods* (*lor*) mutant retina, which produces an abundance of rods but few UV cones, with *Tg(sws1:GFP*). Note the substantial reduction in UV cones in the *lor* mutant retina compared to the wild-type retina. **(C)** UV cone telodendria in *lor* retina. The UV cone telodendria in *lor* mutants appear more tortuous and branched than the UV cone telodendria in wild-type larval retina. **(D)** The number of telodendria per pedicle in the UV cones of the *lor* mutant retinas was reduced by half compared to the wild-type UV cones (Figure 4) ($p<0.0001$, Mann Whitney U test). N=3, 10 pedicles counted/retina. Scale bars in (A) and (B) = 50μm; scale bar in (C) = 20μm.

3 DISCUSSION + FUTURE DIRECTIONS

3.1 Speculation about function of telodendria between short wavelength cones

The role telodendria play in the processing of light information and how they contribute to vision is unclear. It is possible that connections between the short wavelength cones contribute to colour opponency, similar to what occurs in the horizontal cell, to distinguish between wavelengths of light and reduce background. For UV cones, lack of input from blue cones, such as after blue cone ablation, could cause changes in the type of light information processed by the UV cones and allow for compensation. This could contribute to the rapid recovery of visually-mediated behaviour post blue cone ablation [132].

3.2 Telodendria in cells expressing tetanus toxin

Tetanus toxin prevents the movement and formation/fusion of vesicles, and resultantly perturbs the release of neurotransmitters from cells, rendering them unable to communicate with surrounding cells [187]. Tetanus toxin has been expressed in zebrafish photoreceptors to prevent signals from being transmitted to downstream contacts to determine how photoreceptor activity influenced interneuron connectivity [104].

Expressing tetanus toxin within photoreceptors could prevent transmission of factors/signals between photoreceptors. What influence this would have on telodendric connectivity and modification of light information is unknown. If signal transmission is inhibited, the lack of electrical reinforcement could cause the telodendria to degenerate. Expressing tetanus toxin within UV cones and investigating UV cone telodendric connectivity could assess this. If the connections were fewer than that of controls, then the telodendria may be unable to make typical connections due to lack of signal/factor

transmission. Electrophysiology could be used to determine how electrically coupled blue cones respond when the tetanus toxin-expressing UV cone is stimulated. If the connected blue cone does not become activated in a similar way to wild-type, then the tetanus toxin is interfering with cone-cone communication. Alternatively, the lack of input to and from horizontal cells would prevent the appropriate modification of signals between photoreceptors and alter photoreceptor-photoreceptor signalling, even though telodendria may appear normal.

3.3 Cone photoreceptor transplant and telodendria

3.3.1 Transplanted photoreceptor integration into the neural retina

The success of cellular integration post transplant of photoreceptor precursors cells is difficult to assess. Cellular integration is usually determined by migration of the cell into the outer nuclear layer and association with bipolar cells; however, these methods are imprecise and do not characterize whether the newly formed photoreceptors are behaving appropriately and producing functional outputs. Whether the differentiated photoreceptors form typical connections has not been thoroughly determined, and telodendria have been overlooked entirely in this field. For the new photoreceptors to function normally, they must create and maintain connections with cellular partners typical for the photoreceptor type, and that includes telodendric connections with other photoreceptors. Whether the formation of telodendria is occurring would be simple to assess in animal models, especially since introduced photoreceptor precursor cells are often fluorescently labelled. While the formation of telodendria does not equate functionality, it nonetheless would suggest that the cells are properly integrating into the neural retina and forming connections.

3.3.2 Material transfer

Material transfer has been observed in the retina between photoreceptors and introduced photoreceptor precursors [62-65]. Initially, the phenomenon was believed to be the result of cellular fusion between the donor and host cells. Cellular fusion has been observed between stem cells derived from different tissues and in some disease pathologies [188-191]. This confounds assessment of functional integration of cells introduced to a new environment, as the cellular behaviour of fused cells could be different from the surrounding cells. Co-expression of donor and host markers within retinal cells post transplant of donor cells expressing one fluorescent marker into host retina expressing another fluorescent marker could thus be explained by cellular fusion, wherein the original nuclei may remain separate within the shared cell body or also fuse to become a single nuclei [192, 193]. However, in the case of photoreceptor precursor cell transplantation into the retina, cellular fusion was ruled out, as the cells did not appear to have two nuclei [62, 63]. Nuclear fusion was also eliminated as a possibility, due to the absence of polyploidy [62]. Rather, it appears that the donor photoreceptor precursor cells and host cells transfer material to one another. The mechanism behind material transfer is unclear in terms of how the material is transferred and what, specifically, is transferred. DNA was not stably transferred between cells; thus, it appears that RNA or protein is being transferred between the host and donor cells.

The question of what material is being transferred between cells could potentially be addressed using donor cells that have a protein introduced to them, but do not possess the gene for the protein, and therefore cannot make RNA for the protein, and donor cells that do contain the gene, and can thus make RNA and protein. Specifically, the comparison could be made between photoreceptor precursor cells that underwent lipofectin transfection of a purified protein that do not contain the gene for the protein,

with transgenic photoreceptor precursors that possess the protein gene and can make RNA and the protein. If the host cells express the protein after being exposed to transfected donor cells that do not possess the gene, and thus cannot make RNA for the protein, then material transfer can be protein-based and does not rely solely on RNA. Alternatively, if the transgenic cells participate material transfer while the transfected cells do not, it would suggest that RNA is the molecule being transferred between cells, though does not rule out protein transfer.

Telodendria could be a bridge that allows material transfer to occur between donor and host cells in close proximity. Indeed, gap junctions can facilitate movement of small molecules between cells; however, RNA and proteins would be too large to be moved between gap junctions. Material transfer could be achieved through vesicle transport from one cell to another. Telodendria could provide a scaffold for vesicles to be trafficked from one photoreceptor to another, either externally or internally. In primate retina, the junctions at the end of telodendria are ~200-300 nm^2 in size, which has the potential to tolerate internal movement of small vesicles (50-150nm) [144].

Whether telodendria are involved in material transfer is unknown, but as telodendria form contacts between photoreceptor cells, it is possible that the host cell is connecting to the donor cells via telodendric connections and that transfer of components occurs via these bridges. While molecular factors involved in telodendric growth and pathfinding are not known, elucidating these factors could allow for telodendria formation to be inhibited, and how this impacts material transfer to be investigated.

3.4 Telodendria in disease

3.4.1 Gap junction-mediated bystander effect

In retinitis pigmentosa, rods degenerate due to rod-specific lesions while the cones persist for some time. However, the cones nonetheless degenerate eventually, resulting in blindness. The underlying mechanism that leads to cone death in RP is unclear, though it has been speculated that alterations in the microenvironment of the cones, such as the absence of rod-derived cone viability factors, exposure to oxidative stress, and reduced glucose accessibility, could damage the cones after rod degeneration [14-16, 18, 19, 194]. Another potential initiator of cone death could be messages transmitted from the degenerate rods to the healthy cones, via telodendria, resulting in a toxic bystander effect [20]. Gap junctions are known to facilitate bystander effects in this way, wherein the compromised or dying cells send signals to healthy neighbouring cells, triggering cell death pathways [195-197]. This mechanism is referred to as the gap junction-mediated bystander effect.

The gap junction-mediated bystander effect has been found to influence neuronal survivorship after injury. In an *in vitro* model of ischemia, blocking gap junctions decreased the spread of cell death [198]. Similar results were observed in a mouse model of ischemic stroke; pharmacologically blocking or genetically deleting gap junctions prevented the spread of neuronal death in the brain [199]. Blocking gap junctions also protects against the spread of damage in the retina after retinal neuron death in ischemic conditions [200]. Furthermore, in the developing retina, where apoptosis is necessary to establish the stratification of specific cell types and retinal thickness [201-203], gap junction-mediated bystander cell death has been observed, and substances that blocked gap junctions reduced the amount of apoptosis in neighbouring cells [204]. This indicates

that the gap junction-mediated bystander effect is not only detectable in the central nervous system, but occurs in the developing and mature retina.

Telodendric connections between photoreceptors could result in transmission of signals or compounds through gap junctions that instigate cone death in retinitis pigmentosa. Indeed, rods in the human retina have been noted to make connections with cones, and red and green cones in the peripheral retina make connections with other cones or rods [172]. However, what connections macular cones make with other photoreceptors is poorly investigated in humans at this point in time. In macaque retina, foveal cones make more than a dozen connections per pedicle with other cones [162], but whether the cone photoreceptors at the macula periphery are able to connect with rods has not been investigated. If the cones in the peripheral macula that are in proximity to rods primarily connect with other cones and not rods, then this would prevent the gap junction-mediated bystander effect from spreading from the cones to the rods, and could help explain the persistence of peripheral retina in age-related macular degeneration.

Assessment of the gap junction-mediated bystander effect and its influence on cone death in a retinitis pigmentosa model has only been reported once. In two mouse models of RP, cone connexin (Cx36) was deleted and cone health investigated to determine whether loss of cone jap junctions prevented cone death after rod loss [205]. The authors found that cones still degenerated, despite the loss of Cx36 [205]; however, this does not rule out involvement of the gap junction-mediated bystander effect. The rod connexin was still present, and as functional assessment or dye injections were not conducted to determine whether rod-cone coupling was completely abolished, there could still have been transmission of signals or compounds between rods and the cones. The influence of Cx36 loss on cones was also not assessed on its own. Cx36 has complex, contradictory influences on cell survival; Cx36 loss or blockage in the retina has been linked to both

increased vulnerability to injury [206] and neuro-protection [207]. It is possible that the mouse cones could have degenerated due to loss of connexin or an inability to respond to retinal changes, rather than directly due to rod loss. Additionally, the mouse models of RP do not perfectly recapitulate human RP; in the mouse models, rods typically do not develop outer segments, the onset of rod degeneration is rapid, within the first weeks of life. In some lines, rods are almost completely gone by 20 days post birth, before the photoreceptors would have even reached maturity. Additionally, cone persistence after rods begin to die is very brief, if any preservation occurs at all [205, 208-210]. The mouse photoreceptor mosaic is also very different from the human photoreceptor mosaic, which influences the cone micro-environment and photoreceptor-photoreceptor connectivity. Further, it is possible that the gap junction-mediated bystander effect is acting in combination with micro-environmental changes within the retina to result in cone death.

In the mature outer nuclear layer, the gap junction-mediated bystander effect could result in the "point of no return" in photoreceptor disease, where intervention is no longer feasible. It is possible that the remaining islands of seemingly healthy photoreceptors may have already received signals from degenerate cells, triggering the eventual death of the photoreceptor cells that appear healthy. The concept of a point of no return has been of particular concern in gene therapy clinical trials [211], where the participants typically have severe photoreceptor degeneration with islands of functioning cells. At that level of disease progression, intervention may already be too late, and part of the reason for this could be toxic signals transmitted from degenerating photoreceptors to healthy ones through gap junctions.

In conclusion, telodendria have the potential to facilitate gap junction-mediated bystander death in photoreceptor degenerative diseases. The gap junction-mediated

bystander effect is poorly studied in the retina, and its investigation in models of RP could elucidate mechanisms underlying cone death during disease progression.

3.4.2 Telodendric remodelling

Synaptic remodelling is observed in many neurodegenerative diseases. In photoreceptor degenerations, downstream neurons respond to the absence of synaptic input and remodel. There are three stages of remodelling in the retina during RP progression. Phase I begins as rods become dysfunctional, which can be the result of numerous genetic lesions [212, 213]. The rods are not able to renew their outer segments at a typical rate, which also puts the photoreceptors and RPE under stress. At this stage, rods sprout aberrant processes that reach into the inner retina; these processes retract prior to rod death [212, 213]. Rod degeneration starts in late Phase I. In Phase II, cones begin to degenerate; prior to death, cones send ectopic connections to rod bipolar cells [214]. Bipolar cells retract connections with photoreceptors, and can switch synaptic targets from rods to cones in cases where cones are still thriving for a period of time after rod loss. Activated microglia migrate into the outer retina and Müller glia become hypertrophic as the ONL deteriorates, which can create a barrier between the RPE and the remaining neural retina [215, 216]. Phase III involves progressive remodelling. The glial seal becomes bound to the remaining neural retina, and Müller glia cells undergo further hypertrophy and segment the retina. The remaining neurons migrate into atypical positions and form new, aberrant synaptic connections [212].

After loss of connectivity partners, telodendric connections likely deteriorate and remodel. Lack of electrical input could cause the regression of telodendria, and new cellular neighbours could promote growth. Zebrafish would be an excellent model to investigate telodendric remodelling, as they have tools available for targeted ablation of

different photoreceptor types. Specific photoreceptor types can be ablated, and the influence this has on telodendria observed. While this was attempted here in the larval retina, it would be easier to detect in the adult retina, where there is an organized mosaic and the cells are spaced such that branching, length, and cellular partners are more easily determined.

Regenerated cells must wire into the existing neural retina to function; understanding how newly produced cells wire into the pre-existing neural retina is essential for the success of stem cell transplantation therapies. Introduced cells must not only differentiate into the desired cell type, but also integrate in an appropriate and functional manner. After ablating photoreceptors and allowing for regeneration in the adult zebrafish retina, the connectivity of regenerated cells can be assessed. Similarly, how the telodendria of neighbouring photoreceptors remodel and connect with regenerated cells could be observed in the zebrafish retina.

LITERATURE CITED

1. Daiger SP, Sullivan LS, Bowne SJ. Genes and mutations causing retinitis pigmentosa. Clin Genet. 2013;84(2):132-41. doi: 10.1111/cge.12203. PubMed PMID: 23701314; PubMed Central PMCID: PMCPMC3856531.

2. Hamel C. Retinitis pigmentosa. Orphanet J Rare Dis. 2006;1:40. doi: 10.1186/1750-1172-1-40. PubMed PMID: 17032466; PubMed Central PMCID: PMCPMC1621055.

3. Hartong DT, Berson EL, Dryja TP. Retinitis pigmentosa. The Lancet. 2006;368(9549):1795-809. doi: 10.1016/s0140-6736(06)69740-7.

4. Zhang J, Wang C, Shen Y, Chen N, Wang L, Liang L, et al. A mutation in ADIPOR1 causes nonsyndromic autosomal dominant retinitis pigmentosa. Hum Genet. 2016;135(12):1375-87. doi: 10.1007/s00439-016-1730-2. PubMed PMID: 27655171.

5. Beryozkin A, Levy G, Blumenfeld A, Meyer S, Namburi P, Morad Y, et al. Genetic analysis of the rhodopsin gene identifies a mosaic dominant retinitis pigmentosa mutation in a healthy individual. Invest Ophthalmol Vis Sci. 2016;57(3):940-7. doi: 10.1167/iovs.15-18702. PubMed PMID: 26962691; PubMed Central PMCID: PMCPMC4788094.

6. Van Soest S, Westerveld A, De Jong PTVM, Bleeker-Wagemakers EM, Bergen AAB. Retinitis pigmentosa: Defined from a molecular point of view. Survey of Ophthalmology. 1999;43(4):321-34. doi: 10.1016/s0039-6257(98)00046-0.

7. Sung C-H, Chuang JZ. The cell biology of vision. J Cell Biol. 2010;190(6):953-63. doi: 10.1083/jcb.201006020. PubMed PMID: 20855501; PubMed Central PMCID: PMCPMC3101587.

8. Inglehearn CF, Tarttelin EE, Plant C, Peacock RE, Al-Maghtheh M, Vithana E, et al. A linkage survey of 20 dominant retinitis pigmentosa families: frequencies of the nine known loci and evidence for further heterogeneity. Journal of Medical Genetics. 1998;35(1):1-5. doi: DOI 10.1136/jmg.35.1.1. PubMed PMID: WOS:000071636300001; PubMed Central PMCID: PMCPMC1051177.

9. Daiger SP, Rossiter BJF, Greenberg J, Christoffels A, Hide W. Data services and software for identifying genes and mutations causing retinal degeneration. Invest Ophthalmol Vis Sci. 1998;39(S295).

10. Leveillard T, Mohand-Said S, Lorentz O, Hicks D, Fintz AC, Clerin E, et al. Identification and characterization of rod-derived cone viability factor. Nat Genet. 2004;36(7):755-9. doi: 10.1038/ng1386. PubMed PMID: 15220920.

11. Mohand-Said S, Hicks D, Dreyfus H, Sahel JA. Selective transplantation of rods delays cone loss in a retinitis pigmentosa model. Archives of Ophthalmology. 2000;118(6):807. doi: 10.1001/archopht.118.6.807.

12. Yang Y, Mohand-Said S, Danan A, Simonutti M, Fontaine V, Clerin E, et al. Functional cone rescue by RdCVF protein in a dominant model of retinitis pigmentosa. Mol Ther. 2009;17(5):787-95. doi: 10.1038/mt.2009.28. PubMed PMID: 19277021; PubMed Central PMCID: PMCPMC2835133.

13. Byrne LC, Dalkara D, Luna G, Fisher SK, Clerin E, Sahel JA, et al. Viral-mediated RdCVF and RdCVFL expression protects cone and rod photoreceptors in retinal degeneration. J Clin Invest. 2015;125(1):105-16. doi: 10.1172/JCI65654. PubMed PMID: 25415434; PubMed Central PMCID: PMCPMC4382269.

14. Punzo C, Kornacker K, Cepko CL. Stimulation of the insulin/mTOR pathway delays cone death in a mouse model of retinitis pigmentosa. Nat Neurosci. 2009;12(1):44-52. doi: 10.1038/nn.2234. PubMed PMID: 19060896; PubMed Central PMCID: PMCPMC3339764.

15. Venkatesh A, Ma S, Le YZ, Hall MN, Rüegg MA, Punzo C. Activated mTORC1 promotes long-term cone survival in retinitis pigmentosa mice. J Clin Invest. 2015;125(4):1446-58. doi: 10.1172/JCI79766. PubMed PMID: 25798619; PubMed Central PMCID: PMCPMC4396488.

16. Wang W, Lee SJ, Scott PA, Lu X, Emery D, Liu Y, et al. Two-step reactivation of dormant cones in retinitis pigmentosa. Cell Reports. 2016;15(2):372-85. doi: 10.1016/j.celrep.2016.03.022.

17. Yu D-Y, Cringle S, Valter K, Walsh N, Lee D, Stone J. Photoreceptor death, trophic factor expression, retinal oxygen status, and photoreceptor function in the P23H rat. Investigative Opthalmology & Visual Science. 2004;45(6):2013. doi: 10.1167/iovs.03-0845.

18. Komeima K, Rogers BS, Lu L, Campochiaro PA. Antioxidants reduce cone cell death in a model of retinitis pigmentosa. Proc Natl Acad Sci U S A. 2006;103(30):11300-5. doi: 10.1073/pnas.0604056103. PubMed PMID: 16849425; PubMed Central PMCID: PMCPMC1544081.

19. Komeima K, Rogers BS, Campochiaro PA. Antioxidants slow photoreceptor cell death in mouse models of retinitis pigmentosa. J Cell Physiol. 2007;213(3):809-15. doi: 10.1002/jcp.21152. PubMed PMID: 17520694.

20. Ripps H. Cell death in retinitis pigmentosa: gap junctions and the 'bystander' effect. Exp Eye Res. 2002;74(3):327-36. doi: 10.1006/exer.2002.1155. PubMed PMID: 12014914.

21. Chakravarthy U, Wong TY, Fletcher A, Piault E, Evans C, Zlateva G, et al. Clinical risk factors for age-related macular degeneration: a systematic review and meta-analysis. BMC Ophthalmol. 2010;10:31. doi: 10.1186/1471-2415-10-31. PubMed PMID: 21144031; PubMed Central PMCID: PMCPMC3009619.

22. Hageman G, Luthert PL, Chong NHC, Johnson LV, Anderson DH, Mullins RF. An integrated hypothesis that considers drusen as biomarkers of immune-mediated processes at the RPE-Bruch's membrane interface in aging and age-related macular degeneration. Progress in Retinal and Eye Research. 2001;20(6):705-32. doi: 10.1016/s1350-9462(01)00010-6.

23. Mullins RF, Aptsiauri N, Hageman GS. Structure and composition of drusen associated with glomerulonephritis: Implications for the role of complement activation in drusen biogenesis. Eye (Lond). 2001;15(Pt 3):390-5. doi: 10.1038/eye.2001.142. PubMed PMID: 11450763.

24. Johnson LV, Leitner WP, Staples MK, Anderson DH. Complement activation and inflammatory processes in Drusen formation and age related macular degeneration. Exp Eye Res. 2001;73(6):887-96. doi: 10.1006/exer.2001.1094. PubMed PMID: 11846519.

25. Klein RJ, Zeiss C, Chew EY, Tsai JY, Sackler RS, Haynes C, et al. Complement factor H polymorphism in age-related macular degeneration. Science. 2005;308(5720):385-9. doi: 10.1126/science.1109557. PubMed PMID: 15761122; PubMed Central PMCID: PMCPMC1512523.

26. Edwards AO, Ritter R, 3rd, Abel KJ, Manning A, Panhuysen C, Farrer LA. Complement factor H polymorphism and age-related macular degeneration. Science. 2005;308(5720):421-4. doi: 10.1126/science.1110189. PubMed PMID: 15761121.

27. Haines JL, Hauser MA, Schmidt S, Scott WK, Olson LM, Gallins P, et al. Complement factor H variant increases the risk of age-related macular degeneration. Science. 2005;308(5720):419-21. doi: 10.1126/science.1110359. PubMed PMID: 15761120.

28. Fritsche LG, Chen W, Schu M, Yaspan BL, Yu Y, Thorleifsson G, et al. Seven new loci associated with age-related macular degeneration. Nat Genet. 2013;45(4):433-9, 9e1-2. doi: 10.1038/ng.2578. PubMed PMID: 23455636; PubMed Central PMCID: PMCPMC3739472.

29. Fagerness JA, Maller JB, Neale BM, Reynolds RC, Daly MJ, Seddon JM. Variation near complement factor I is associated with risk of advanced AMD. Eur J Hum Genet. 2009;17(1):100-4. doi: 10.1038/ejhg.2008.140. PubMed PMID: 18685559; PubMed Central PMCID: PMCPMC2985963.

30. Fritsche LG, Igl W, Bailey JN, Grassmann F, Sengupta S, Bragg-Gresham JL, et al. A large genome-wide association study of age-related macular degeneration highlights contributions of rare and common variants. Nat Genet. 2016;48(2):134-43. doi: 10.1038/ng.3448. PubMed PMID: 26691988; PubMed Central PMCID: PMCPMC4745342.

31. Gold B, Merriam JE, Zernant J, Hancox LS, Taiber AJ, Gehrs K, et al. Variation in factor B (BF) and complement component 2 (C2) genes is associated with age-related macular degeneration. Nat Genet. 2006;38(4):458-62. doi: 10.1038/ng1750. PubMed PMID: 16518403; PubMed Central PMCID: PMCPMC2921703.

32. Maller JB, Fagerness JA, Reynolds RC, Neale BM, Daly MJ, Seddon JM. Variation in complement factor 3 is associated with risk of age-related macular degeneration. Nat Genet. 2007;39(10):1200-1. doi: 10.1038/ng2131. PubMed PMID: 17767156.

33. Yates JR, Sepp T, Matharu BK, Khan JC, Thurlby DA, Shahid H, et al. Complement C3 variant and the risk of age-related macular degeneration. N Engl J Med. 2007;357(6):553-61. doi: 10.1056/NEJMoa072618. PubMed PMID: 17634448.

34. Geerlings MJ, de Jong EK, den Hollander AI. The complement system in age-related macular degeneration: A review of rare genetic variants and implications for personalized treatment. Mol Immunol. 2017;84:65-76. doi: 10.1016/j.molimm.2016.11.016. PubMed PMID: 27939104; PubMed Central PMCID: PMCPMC5380947.

35. van Lookeren Campagne M, Strauss EC, Yaspan BL. Age-related macular degeneration: Complement in action. Immunobiology. 2016;221(6):733-9. doi: 10.1016/j.imbio.2015.11.007. PubMed PMID: 26742632.

36. Mussolino C, della Corte M, Rossi S, Viola F, Di Vicino U, Marrocco E, et al. AAV-mediated photoreceptor transduction of the pig cone-enriched retina. Gene Therapy. 2011;18(7):637-45. doi: 10.1038/gt.2011.3.
37. Trapani I, Puppo A, Auricchio A. Vector platforms for gene therapy of inherited retinopathies. Prog Retin Eye Res. 2014;43:108-28. doi: 10.1016/j.preteyeres.2014.08.001. PubMed PMID: 25124745; PubMed Central PMCID: PMCPMC4241499.
38. Palfi S, Gurruchaga JM, Ralph GS, Lepetit H, Lavisse S, Buttery PC, et al. Long-term safety and tolerability of ProSavin, a lentiviral vector-based gene therapy for Parkinson's disease: a dose escalation, open-label, phase 1/2 trial. The Lancet. 2014;383(9923):1138-46. doi: 10.1016/s0140-6736(13)61939-x.
39. Kong J, Kim SR, Binley K, Pata I, Doi K, Mannik J, et al. Correction of the disease phenotype in the mouse model of Stargardt disease by lentiviral gene therapy. Gene Ther. 2008;15(19):1311-20. doi: 10.1038/gt.2008.78. PubMed PMID: 18463687; PubMed Central PMCID: PMCPMC3110063.
40. Binley K, Widdowson P, Loader J, Kelleher M, Iqball S, Ferrige G, et al. Transduction of photoreceptors with equine infectious anemia virus lentiviral vectors: safety and biodistribution of StarGen for Stargardt disease. Invest Ophthalmol Vis Sci. 2013;54(6):4061-71. doi: 10.1167/iovs.13-11871. PubMed PMID: 23620430; PubMed Central PMCID: PMCPMC3681475.
41. Bainbridge JW, Smith AJ, Barker SS, Robbie S, Henderson R, Balaggan K, et al. Effect of gene therapy on visual function in Leber's congenital amaurosis. N Engl J Med. 2008;358(21):2231-9. doi: 10.1056/NEJMoa0802268. PubMed PMID: 18441371.
42. Cideciyan AV, Hauswirth WW, Aleman TS, Kaushal S, Schwartz SB, Boye SL, et al. Human RPE65 gene therapy for Leber congenital amaurosis: persistence of early visual improvements and safety at 1 year. Hum Gene Ther. 2009;20(9):999-1004. doi: 10.1089/hum.2009.086. PubMed PMID: 19583479; PubMed Central PMCID: PMCPMC2829287.
43. Hauswirth WW, Aleman TS, Kaushal S, Cideciyan AV, Schwartz SB, Wang L, et al. Treatment of leber congenital amaurosis due to RPE65 mutations by ocular subretinal injection of adeno-associated virus gene vector: short-term results of a phase I trial. Hum Gene Ther. 2008;19(10):979-90. doi: 10.1089/hum.2008.107. PubMed PMID: 18774912; PubMed Central PMCID: PMCPMC2940541.

44. Jacobson SG, Cideciyan AV, Ratnakaram R, Heon E, Schwartz SB, Roman AJ, et al. Gene therapy for leber congenital amaurosis caused by RPE65 mutations: safety and efficacy in 15 children and adults followed up to 3 years. Arch Ophthalmol. 2012;130(1):9-24. doi: 10.1001/archophthalmol.2011.298. PubMed PMID: 21911650; PubMed Central PMCID: PMCPMC3600816.

45. Maguire AM, Simonelli F, Pierce EA, Pugh EN, Jr., Mingozzi F, Bennicelli J, et al. Safety and efficacy of gene transfer for Leber's congenital amaurosis. N Engl J Med. 2008;358(21):2240-8. doi: 10.1056/NEJMoa0802315. PubMed PMID: 18441370; PubMed Central PMCID: PMCPMC2829748.

46. Takahashi K, Tanabe K, Ohnuki M, Narita M, Ichisaka T, Tomoda K, et al. Induction of pluripotent stem cells from adult human fibroblasts by defined factors. Cell. 2007;131(5):861-72. doi: 10.1016/j.cell.2007.11.019. PubMed PMID: 18035408.

47. Takahashi K, Yamanaka S. Induction of pluripotent stem cells from mouse embryonic and adult fibroblast cultures by defined factors. Cell. 2006;126(4):663-76. doi: 10.1016/j.cell.2006.07.024. PubMed PMID: 16904174.

48. Yu J, Vodyanik MA, Smuga-Otto K, Antosiewicz-Bourget J, Frane JL, Tian S, et al. Induced pluripotent stem cell lines derived from human somatic cells. Science. 2007;318(5858):1917-20. doi: 10.1126/science.1151526. PubMed PMID: 18029452.

49. Zhou L, Wang W, Liu Y, de Castro JF, Ezashi T, Telugu BPVL, et al. Differentiation of induced pluripotent stem cells of swine into rod photoreceptors and their integration into the retina. Stem Cells. 2011;29(6):972-80. doi: 10.1002/stem.637.

50. Eiraku M, Takata N, Ishibashi H, Kawada M, Sakakura E, Okuda S, et al. Self-organizing optic-cup morphogenesis in three-dimensional culture. Nature. 2011;472(7341):51-6. doi: 10.1038/nature09941. PubMed PMID: 21475194.

51. Volkner M, Zschatzsch M, Rostovskaya M, Overall RW, Busskamp V, Anastassiadis K, et al. Retinal Organoids from Pluripotent Stem Cells Efficiently Recapitulate Retinogenesis. Stem Cell Reports. 2016;6(4):525-38. doi: 10.1016/j.stemcr.2016.03.001. PubMed PMID: 27050948; PubMed Central PMCID: PMCPMC4834051.

52. Hiler D, Chen X, Hazen J, Kupriyanov S, Carroll PA, Qu C, et al. Quantification of Retinogenesis in 3D Cultures Reveals Epigenetic Memory and Higher Efficiency in iPSCs Derived from Rod Photoreceptors. Cell Stem Cell. 2015;17(1):101-15. doi:

10.1016/j.stem.2015.05.015. PubMed PMID: 26140606; PubMed Central PMCID: PMCPMC4547539.

53. Zhong X, Gutierrez C, Xue T, Hampton C, Vergara MN, Cao LH, et al. Generation of three-dimensional retinal tissue with functional photoreceptors from human iPSCs. Nat Commun. 2014;5:4047. doi: 10.1038/ncomms5047. PubMed PMID: 24915161; PubMed Central PMCID: PMCPMC4370190.

54. Pearson RA, Barber AC, Rizzi M, Hippert C, Xue T, West EL, et al. Restoration of vision after transplantation of photoreceptors. Nature. 2012;485(7396):99-103. doi: 10.1038/nature10997. PubMed PMID: 22522934; PubMed Central PMCID: PMCPMC3888831.

55. MacLaren RE, Pearson RA, MacNeil A, Douglas RH, Salt TE, Akimoto M, et al. Retinal repair by transplantation of photoreceptor precursors. Nature. 2006;444(7116):203-7. doi: 10.1038/nature05161.

56. Lakowski J, Baron M, Bainbridge J, Barber AC, Pearson RA, Ali RR, et al. Cone and rod photoreceptor transplantation in models of the childhood retinopathy Leber congenital amaurosis using flow-sorted Crx-positive donor cells. Hum Mol Genet. 2010;19(23):4545-59. doi: 10.1093/hmg/ddq378. PubMed PMID: 20858907; PubMed Central PMCID: PMCPMC2972691.

57. Klassen H, Kiilgaard JF, Zahir T, Ziaeian B, Kirov I, Scherfig E, et al. Progenitor cells from the porcine neural retina express photoreceptor markers after transplantation to the subretinal space of allorecipients. Stem Cells. 2007;25(5):1222-30. doi: 10.1634/stemcells.2006-0541. PubMed PMID: 17218397.

58. Wang W, Zhou L, Lee SJ, Liu Y, Fernandez de Castro J, Emery D, et al. Swine cone and rod precursors arise sequentially and display sequential and transient integration and differentiation potential following transplantation. Investigative Opthalmology & Visual Science. 2014;55(1):301. doi: 10.1167/iovs.13-12600.

59. Lamba DA, Gust J, Reh TA. Transplantation of human embryonic stem cell-derived photoreceptors restores some visual function in Crx-deficient mice. Cell Stem Cell. 2009;4(1):73-9. doi: 10.1016/j.stem.2008.10.015. PubMed PMID: 19128794; PubMed Central PMCID: PMCPMC2713676.

60. Homma K, Okamoto S, Mandai M, Gotoh N, Rajasimha HK, Chang YS, et al. Developing rods transplanted into the degenerating retina of Crx-knockout mice exhibit neural activity similar to native photoreceptors. Stem Cells. 2013;31(6):1149-59. doi:

10.1002/stem.1372. PubMed PMID: 23495178; PubMed Central PMCID: PMCPMC4540234.

61. Eberle D, Schubert S, Postel K, Corbeil D, Ader M. Increased integration of transplanted CD73-positive photoreceptor precursors into adult mouse retina. Investigative Opthalmology & Visual Science. 2011;52(9):6462. doi: 10.1167/iovs.11-7399.

62. Pearson RA, Gonzalez-Cordero A, West EL, Ribeiro JR, Aghaizu N, Goh D, et al. Donor and host photoreceptors engage in material transfer following transplantation of post-mitotic photoreceptor precursors. Nature Communications. 2016;7:13029. doi: 10.1038/ncomms13029.

63. Santos-Ferreira T, Llonch S, Borsch O, Postel K, Haas J, Ader M. Retinal transplantation of photoreceptors results in donor–host cytoplasmic exchange. Nature Communications. 2016;7:13028. doi: 10.1038/ncomms13028.

64. Singh MS, Balmer J, Barnard AR, Aslam SA, Moralli D, Green CM, et al. Transplanted photoreceptor precursors transfer proteins to host photoreceptors by a mechanism of cytoplasmic fusion. Nat Commun. 2016;7:13537. doi: 10.1038/ncomms13537. PubMed PMID: 27901042; PubMed Central PMCID: PMCPMC5141374.

65. Ortin-Martinez A, Tsai EL, Nickerson PE, Bergeret M, Lu Y, Smiley S, et al. A reinterpretation of cell transplantation: GFP transfer from donor to host photoreceptors. Stem Cells. 2017;35(4):932-9. doi: 10.1002/stem.2552. PubMed PMID: 27977075.

66. Horvath P, Barrangou R. CRISPR/Cas, the immune system of bacteria and archaea. Science. 2010;327(5962):167-70. doi: 10.1126/science.1179555. PubMed PMID: 20056882.

67. Cong L, Ran FA, Cox D, Lin S, Barretto R, Habib N, et al. Multiplex genome engineering using CRISPR/Cas systems. Science. 2013;339(6121):819-23. doi: 10.1126/science.1231143. PubMed PMID: 23287718; PubMed Central PMCID: PMCPMC3795411.

68. Yu W, Mookherjee S, Chaitankar V, Hiriyanna S, Kim JW, Brooks M, et al. Nrl knockdown by AAV-delivered CRISPR/Cas9 prevents retinal degeneration in mice. Nat Commun. 2017;8:14716. doi: 10.1038/ncomms14716. PubMed PMID: 28291770; PubMed Central PMCID: PMCPMC5355895.

69. Hung SS, Chrysostomou V, Li F, Lim JK, Wang JH, Powell JE, et al. AAV-Mediated CRISPR/Cas Gene Editing of Retinal Cells In Vivo. Invest Ophthalmol Vis Sci. 2016;57(7):3470-6. doi: 10.1167/iovs.16-19316. PubMed PMID: 27367513.

70. Mears AJ, Kondo M, Swain PK, Takada Y, Bush RA, Saunders TL, et al. Nrl is required for rod photoreceptor development. Nat Genet. 2001;29(4):447-52. doi: 10.1038/ng774. PubMed PMID: 11694879.

71. Schmitt EA, Hyatt GA, Dowling JE. Erratum: Temporal and spatial patterns of opsin gene expression in the zebrafish (Danio rerio): corrections with additions. Vis Neurosci. 1999;16(3):601-5. PubMed PMID: 10349978.

72. Neuhauss SC. Behavioral genetic approaches to visual system development and function in zebrafish. J Neurobiol. 2003;54(1):148-60. doi: 10.1002/neu.10165. PubMed PMID: 12486702.

73. Raymond PA, Barthel LK, Rounsifer ME, Sullivan SA, Knight JK. Expression of rod and cone visual pigments in goldfish and zebrafish: A rhodopsin-like gene is expressed in cones. Neuron. 1993;10(6):1161-74. doi: Doi 10.1016/0896-6273(93)90064-X. PubMed PMID: WOS:A1993LK37300016.

74. Raymond PA, Barthel LK, Stenkamp DL. The zebrafish ultraviolet cone opsin reported previously is expressed in rods. Investigative Ophthalmology & Visual Science. 1996;37(5):948-50. PubMed PMID: WOS:A1996UD85300029.

75. Allison WT, Haimberger TJ, Hawryshyn CW, Temple SE. Visual pigment composition in zebrafish: Evidence for a rhodopsin-porphyropsin interchange system. Vis Neurosci. 2004;21(6):945-52. doi: 10.1017/S0952523804216145. PubMed PMID: 15733349.

76. Vihtelic TS, Doro CJ, Hyde DR. Cloning and characterization of six zebrafish photoreceptor opsin cDNAs and immunolocalization of their corresponding proteins. Visual Neuroscience. 1999;16(3):571-85. PubMed PMID: WOS:000080234000016.

77. Chinen A, Hamaoka T, Yamada Y, Kawamura S. Gene duplication and spectral diversification of cone visual pigments of zebrafish. Genetics. 2003;163(2):663-75. PubMed PMID: 12618404; PubMed Central PMCID: PMCPMC1462461.

78. Allison WT, Barthel LK, Skebo KM, Takechi M, Kawamura S, Raymond PA. Ontogeny of cone photoreceptor mosaics in zebrafish. J Comp Neurol. 2010;518(20):4182-95. doi: 10.1002/cne.22447. PubMed PMID: 20878782; PubMed Central PMCID: PMCPMC3376642.

79. Engström K. Cone types and cone arrangements in the retina of some cyprinids. Acta Zool. 1960;41:227-95.
80. Engström K. Cone types and cone arrangements in teleost retinae. Acta Zool. 1963;44:179-243.
81. Raymond PA, Barthel LK. A moving wave patterns the cone photoreceptor mosaic array in the zebrafish retina. Int J Dev Biol. 2004;48(8-9):935-45. doi: 10.1387/ijdb.041873pr. PubMed PMID: 15558484.
82. Viets K, Eldred KC, Johnston RJ, Jr. Mechanisms of photoreceptor patterning in vertebrates and invertebrates. Trends Genet. 2016;32(10):638-59. doi: 10.1016/j.tig.2016.07.004. PubMed PMID: 27615122; PubMed Central PMCID: PMCPMC5035628.
83. Copenhagen DR, Owen WG. Functional characteristics of lateral interactions between rods in the retina of the snapping turtle. The Journal of Physiology. 1976;259(2):251-82. doi: 10.1113/jphysiol.1976.sp011465.
84. Jackman SL, Babai N, Chambers JJ, Thoreson WB, Kramer RH. A positive feedback synapse from retinal horizontal cells to cone photoreceptors. PLoS Biol. 2011;9(5):e1001057. doi: 10.1371/journal.pbio.1001057. PubMed PMID: 21559323; PubMed Central PMCID: PMCPMC3086870.
85. Ohtsuka T, Kawamata K. Telodendrial contact of HRP-filled photoreceptors in the turtle retina: pathways of photoreceptor coupling. J Comp Neurol. 1990;292(4):599-613. doi: 10.1002/cne.902920409. PubMed PMID: 2324315.
86. Owen WG. Chemical and electrical synapses between photoreceptors in the retina of the turtle, Chelydra serpentina. J Comp Neurol. 1985;240(4):423-33. doi: 10.1002/cne.902400410. PubMed PMID: 2468693.
87. Thoreson WB, Mangel SC. Lateral interactions in the outer retina. Prog Retin Eye Res. 2012;31(5):407-41. doi: 10.1016/j.preteyeres.2012.04.003. PubMed PMID: 22580106; PubMed Central PMCID: PMCPMC3401171.
88. Warren TJ, Van Hook MJ, Tranchina D, Thoreson WB. Kinetics of Inhibitory Feedback from Horizontal Cells to Photoreceptors: Implications for an Ephaptic Mechanism. J Neurosci. 2016;36(39):10075-88. doi: 10.1523/JNEUROSCI.1090-16.2016. PubMed PMID: 27683904; PubMed Central PMCID: PMCPMC5039255.
89. O'Brien J, Nguyen HB, Mills SL. Cone photoreceptors in bass retina use two connexins to mediate electrical coupling. J Neurosci. 2004;24(24):5632-42. doi:

10.1523/JNEUROSCI.1248-04.2004. PubMed PMID: 15201336; PubMed Central PMCID: PMCPMC2222551.

90. Kamermans M, Kraaij DA, Spekreijse H. The cone/horizontal cell network: a possible site for color constancy. Vis Neurosci. 1998;15(5):787-97. PubMed PMID: 9764521.

91. Packer OS, Verweij J, Li PH, Schnapf JL, Dacey DM. Blue-yellow opponency in primate S cone photoreceptors. J Neurosci. 2010;30(2):568-72. doi: 10.1523/JNEUROSCI.4738-09.2010. PubMed PMID: 20071519; PubMed Central PMCID: PMCPMC2826135.

92. Chapot CA, Euler T, Schubert T. How do horizontal cells "talk" to cone photoreceptors? Different levels of complexity at the cone-horizontal cell synapse. J Physiol. 2017. doi: 10.1113/JP274177. PubMed PMID: 28378516.

93. Vroman R, Klaassen LJ, Howlett MH, Cenedese V, Klooster J, Sjoerdsma T, et al. Extracellular ATP hydrolysis inhibits synaptic transmission by increasing ph buffering in the synaptic cleft. PLoS Biol. 2014;12(5):e1001864. doi: 10.1371/journal.pbio.1001864. PubMed PMID: 24844296; PubMed Central PMCID: PMCPMC4028192.

94. Peichl L, González-Soriano J. Morphological types of horizontal cell in rodent retinae: A comparison of rat, mouse, gerbil, and guinea pig. Visual Neuroscience. 2009;11(03):501-17. doi: 10.1017/s095252380000242x.

95. Dacey DM, Lee BB, Stafford DK, Pokorny J, Smith VC. Horizontal cells of the primate retina: Cone specificity without spectral opponency. Science. 1996;271(5249):656-9. doi: 10.1126/science.271.5249.656.

96. Ahnelt P, Kolb H. Horizontal cells and cone photoreceptors in human retina: A Golgi-electron microscopic study of spectral connectivity. J Comp Neurol. 1994;343(3):406-27. doi: 10.1002/cne.903430306. PubMed PMID: 8027450.

97. Ahnelt P, Kolb H. Horizontal cells and cone photoreceptors in primate retina: A Golgi-light microscopic study of spectral connectivity. J Comp Neurol. 1994;343(3):387-405. doi: 10.1002/cne.903430305. PubMed PMID: 8027449.

98. Chan TL, Grünert U. Horizontal cell connections with short wavelength-sensitive cones in the retina: A comparison between New World and Old World primates. The Journal of Comparative Neurology. 1998;393(2):196-209. doi: 10.1002/(sici)1096-9861(19980406)393:2<196::aid-cne5>3.0.co;2-y.

99. Goodchild AK, Chan TL, Grünert U. Horizontal cell connections with short-wavelength-sensitive cones in macaque monkey retina. Visual Neuroscience. 1996;13(05):833-45. doi: 10.1017/s0952523800009093.
100. Klaassen LJ, de Graaff W, van Asselt JB, Klooster J, Kamermans M. Specific connectivity between photoreceptors and horizontal cells in the zebrafish retina. J Neurophysiol. 2016;116(6):2799-814. doi: 10.1152/jn.00449.2016. PubMed PMID: 27707811; PubMed Central PMCID: PMCPMC5155036.
101. Li YN, Matsui JI, Dowling JE. Specificity of the horizontal cell-photoreceptor connections in the zebrafish (Danio rerio) retina. J Comp Neurol. 2009;516(5):442-53. doi: 10.1002/cne.22135. PubMed PMID: 19655401; PubMed Central PMCID: PMCPMC2841349.
102. Song PI, Matsui JI, Dowling JE. Morphological types and connectivity of horizontal cells found in the adult zebrafish (Danio rerio) retina. J Comp Neurol. 2008;506(2):328-38. doi: 10.1002/cne.21549. PubMed PMID: 18022944; PubMed Central PMCID: PMCPMC2408720.
103. Yoshimatsu T, D'Orazi FD, Gamlin CR, Suzuki SC, Suli A, Kimelman D, et al. Presynaptic partner selection during retinal circuit reassembly varies with timing of neuronal regeneration in vivo. Nat Commun. 2016;7:10590. doi: 10.1038/ncomms10590. PubMed PMID: 26838932; PubMed Central PMCID: PMCPMC4742908.
104. Yoshimatsu T, Williams PR, D'Orazi FD, Suzuki SC, Fadool JM, Allison WT, et al. Transmission from the dominant input shapes the stereotypic ratio of photoreceptor inputs onto horizontal cells. Nat Commun. 2014;5:3699. doi: 10.1038/ncomms4699. PubMed PMID: 24832361; PubMed Central PMCID: PMCPMC4061492.
105. Schultze M. Zur Anatomie and Physiologie der Retina Ach mikr Anat 1866;2. Epub 286.
106. Cajal SRY. La retine des vertebres. Translation in R.W. Rodieck, The Vertebrate Retina: Principles of Structure and Function (1973). San Francisco: Freeman Press. 1893.
107. Normann RA, Perlman I, Daly SJ. Mixing of color signals by turtle cone photoreceptors. J Neurophysiol. 1985;54(2):293-303. PubMed PMID: 4031989.
108. Normann RA, Perlman I, Kolb H, Jones J, Daly S. Direct excitatory interactions between cones of different spectral types in the turtle retina. Science. 1984;224(4649):625-7. doi: 10.1126/science.6710161.

109. Lamb TD, Simon EJ. The relation between intercellular coupling and electrical noise in turtle photoreceptors. J Physiology. 1976;263(2):257-86. doi: 10.1113/jphysiol.1976.sp011631.

110. DeVries SHQ, X.; Smith, R.; Makous, W.; Sterling, P. . Electrical coupling between mammalian cones. Current Biology. 2002;12(22):1900-7. doi: 10.1016/S0960-9822(02)01261-7.

111. Firsov ML, Green DG. Photoreceptor coupling in turtle retina. Vis Neurosci. 1998;15(4):755-64. PubMed PMID: 9682876.

112. Attwell D, Wilson M, Wu SM. The effect of light on the spread of signals through the rod network of the salamander retina. Brain Research. 1985;343(1):79-88. doi: 10.1016/0006-8993(85)91160-6.

113. Cameron DA. Cellular proliferation and neurogenesis in the injured retina of adult zebrafish. Vis Neurosci. 2000;17(5):789-97. PubMed PMID: 11153658.

114. Curado S, Stainier DY, Anderson RM. Nitroreductase-mediated cell/tissue ablation in zebrafish: a spatially and temporally controlled ablation method with applications in developmental and regeneration studies. Nat Protoc. 2008;3(6):948-54. doi: 10.1038/nprot.2008.58. PubMed PMID: 18536643; PubMed Central PMCID: PMCPMC2705989.

115. DuVal MG, Chung H, Lehmann OJ, Allison WT. Longitudinal fluorescent observation of retinal degeneration and regeneration in zebrafish using fundus lens imaging. Mol Vis. 2013;19:1082-95. PubMed PMID: 23734077; PubMed Central PMCID: PMCPMC3668685.

116. Fimbel SM, Montgomery JE, Burket CT, Hyde DR. Regeneration of inner retinal neurons after intravitreal injection of ouabain in zebrafish. J Neurosci. 2007;27(7):1712-24. doi: 10.1523/JNEUROSCI.5317-06.2007. PubMed PMID: 17301179.

117. Fischer AJ, Bosse JL, El-Hodiri HM. The ciliary marginal zone (CMZ) in development and regeneration of the vertebrate eye. Exp Eye Res. 2013;116:199-204. doi: 10.1016/j.exer.2013.08.018. PubMed PMID: 24025744.

118. Fleisch VC, Fraser B, Allison WT. Investigating regeneration and functional integration of CNS neurons: lessons from zebrafish genetics and other fish species. Biochim Biophys Acta. 2011;1812(3):364-80. doi: 10.1016/j.bbadis.2010.10.012. PubMed PMID: 21044883.

119. Fraser B, DuVal MG, Wang H, Allison WT. Regeneration of cone photoreceptors when cell ablation is primarily restricted to a particular cone subtype. PLoS One. 2013;8(1):e55410. doi: 10.1371/journal.pone.0055410. PubMed PMID: 23383182; PubMed Central PMCID: PMCPMC3559598.
120. Gorsuch RA, Hyde DR. Regulation of Muller glial dependent neuronal regeneration in the damaged adult zebrafish retina. Exp Eye Res. 2014;123:131-40. doi: 10.1016/j.exer.2013.07.012. PubMed PMID: 23880528; PubMed Central PMCID: PMCPMC3877724.
121. Nagashima M, Barthel LK, Raymond PA. A self-renewing division of zebrafish Muller glial cells generates neuronal progenitors that require N-cadherin to regenerate retinal neurons. Development. 2013;140(22):4510-21. doi: 10.1242/dev.090738. PubMed PMID: 24154521; PubMed Central PMCID: PMCPMC3817940.
122. Thummel R, Kassen SC, Enright JM, Nelson CM, Montgomery JE, Hyde DR. Characterization of Müller glia and neuronal progenitors during adult zebrafish retinal regeneration. Experimental Eye Research. 2008;87(5):433-44. doi: 10.1016/j.exer.2008.07.009.
123. Vihtelic TS, Hyde DR. Light-induced rod and cone cell death and regeneration in the adultalbino zebrafish (Danio rerio) retina. Journal of Neurobiology. 2000;44(3):289-307. doi: 10.1002/1097-4695(20000905)44:3<289::aid-neu1>3.0.co;2-h.
124. Yurco P, Cameron DA. Responses of Muller glia to retinal injury in adult zebrafish. Vision Res. 2005;45(8):991-1002. doi: 10.1016/j.visres.2004.10.022. PubMed PMID: 15695184.
125. Wan Y, Almeida AD, Rulands S, Chalour N, Muresan L, Wu Y, et al. The ciliary marginal zone of the zebrafish retina: clonal and time-lapse analysis of a continuously growing tissue. Development. 2016;143(7):1099-107. doi: 10.1242/dev.133314. PubMed PMID: 26893352; PubMed Central PMCID: PMCPMC4852496.
126. Fausett BV, Goldman D. A role for alpha1 tubulin-expressing Muller glia in regeneration of the injured zebrafish retina. J Neurosci. 2006;26(23):6303-13. doi: 10.1523/JNEUROSCI.0332-06.2006. PubMed PMID: 16763038.
127. Bhatia B, Singhal S, Lawrence JM, Khaw PT, Limb GA. Distribution of Muller stem cells within the neural retina: evidence for the existence of a ciliary margin-like zone in the adult human eye. Exp Eye Res. 2009;89(3):373-82. doi: 10.1016/j.exer.2009.04.005. PubMed PMID: 19379736.

128. Lawrence JM, Singhal S, Bhatia B, Keegan DJ, Reh TA, Luthert PJ, et al. MIO-M1 cells and similar muller glial cell lines derived from adult human retina exhibit neural stem cell characteristics. Stem Cells. 2007;25(8):2033-43. doi: 10.1634/stemcells.2006-0724. PubMed PMID: 17525239.

129. Giannelli SG, Demontis GC, Pertile G, Rama P, Broccoli V. Adult human Muller glia cells are a highly efficient source of rod photoreceptors. Stem Cells. 2011;29(2):344-56. doi: 10.1002/stem.579. PubMed PMID: 21732491.

130. Jayaram H, Jones MF, Eastlake K, Cottrill PB, Becker S, Wiseman J, et al. Transplantation of photoreceptors derived from human Muller glia restore rod function in the P23H rat. Stem Cells Transl Med. 2014;3(3):323-33. doi: 10.5966/sctm.2013-0112. PubMed PMID: 24477073; PubMed Central PMCID: PMCPMC3952927.

131. White DT, Mumm JS. The nitroreductase system of inducible targeted ablation facilitates cell-specific regenerative studies in zebrafish. Methods. 2013;62(3):232-40. doi: 10.1016/j.ymeth.2013.03.017.

132. Hagerman GF, Noel NCL, Cao SY, DuVal MG, Oel AP, Allison WT. Rapid Recovery of Visual Function Associated with Blue Cone Ablation in Zebrafish. Plos One. 2016;11(11):e0166932. doi: 10.1371/journal.pone.0166932.

133. Shahinfar S, Edward DP, Tso MO. A pathological study of photoreceptor cell death in retinal photic injury. Curr Eye Res. 1991;10(1):47-59.

134. Penn JS. Effects of continuous light on the retina of a fish, Notemigonus crysoleucas. J Comp Neurol. 1985;238(1):121-7. doi: 10.1002/cne.902380111. PubMed PMID: 4044903.

135. Marotte LR, Wye-Dvorak J, Mark RF. Retinotectal reorganization in goldfish - II. Effects of partial tectal ablation and constant light on the retina. Neurosci. 1979;4(6):803-10.

136. Mensinger AF, Powers MK. Visual function in regenerating teleost retina following surgical lesioning. Vis Neurosci. 2007;24(3):299-307. doi: 10.1017/S0952523807070265. PubMed PMID: 17550640.

137. Hitchcock PF, Cirenza P. Synaptic organization of regenerated retina in the goldfish. J Comp Neurol. 1994;343(4):609-16. doi: 10.1002/cne.903430410. PubMed PMID: 8034791.

138. Cameron DA, Easter SS, Jr. Cone photoreceptor regeneration in adult fish retina: phenotypic determination and mosaic pattern formation. J Neurosci. 1995;15(3 Pt 2):2255-71. PubMed PMID: 7891164.

139. Maier W, Wolburg H. Regeneration of the goldfish retina after exposure to different doses of ouabain. Cell Tissue Res. 1979;202(1):99-118. PubMed PMID: 509506.

140. Morris AC, Schroeter EH, Bilotta J, Wong RO, Fadool JM. Cone survival despite rod degeneration in XOPS-mCFP transgenic zebrafish. Invest Ophthalmol Vis Sci. 2005;46(12):4762-71. doi: 10.1167/iovs.05-0797. PubMed PMID: 16303977; PubMed Central PMCID: PMCPMC2810103.

141. Vroman R, Klaassen LJ, Kamermans M. Ephaptic communication in the vertebrate retina. Front Hum Neurosci. 2013;7:612. doi: 10.3389/fnhum.2013.00612. PubMed PMID: 24068997; PubMed Central PMCID: PMCPMC3780359.

142. Kolb H. The organization of the outer plexiform layer in the retina of the cat: electron microscopic observations. J Neurocytol. 1977;6(2):131-53. PubMed PMID: 856949.

143. Li H, Chuang AZ, O'Brien J. Photoreceptor coupling is controlled by connexin 35 phosphorylation in zebrafish retina. J Neurosci. 2009;29(48):15178-86. doi: 10.1523/JNEUROSCI.3517-09.2009. PubMed PMID: 19955370; PubMed Central PMCID: PMCPMC2909833.

144. O'Brien JJ, Chen X, Macleish PR, O'Brien J, Massey SC. Photoreceptor coupling mediated by connexin36 in the primate retina. J Neurosci. 2012;32(13):4675-87. doi: 10.1523/JNEUROSCI.4749-11.2012. PubMed PMID: 22457514; PubMed Central PMCID: PMCPMC3335500.

145. Goede P, Kolb H. Three-dimensional reconstruction and surface rendering of the five different spectral types of cone pedicle in the turtle retina. J Neurosci Methods. 1995;62(1-2):83-8. PubMed PMID: 8750088.

146. Kolb H, Jones J. Electron-Microscopy of Golgi-Impregnated Photoreceptors Reveals Connections between Red and Green Cones in the Turtle Retina. Journal of Neurophysiology. 1985;54(2):304-17. PubMed PMID: WOS:A1985ANY3000009.

147. Kolb H, Jones J. Synaptic organization of the outer plexiform layer of the turtle retina: an electron microscope study of serial sections. J Neurocytol. 1984;13(4):567-91. PubMed PMID: 6481412.

148. Detwiler PB, Hodgkin AL. Electrical coupling between cones in turtle retina. The Journal of Physiology. 1979;291(1):75-100. doi: 10.1113/jphysiol.1979.sp012801.
149. Baylor DA, Fuortes MGF, O'Bryan PM. Receptive fields of cones in the retina of the turtle. J of Physiology. 1971;214(2):265-94. doi: 10.1113/jphysiol.1971.sp009432.
150. Copenhagen DR, Owen WG. Coupling between rod photoreceptors in a vertebrate retina. Nature 1976;260.
151. Gold GH, Dowling JE. Photoreceptor coupling in retina of the toad, Bufo marinus. I. Anatomy. . J Neurophyiol. 1979.
152. Zhang J, Wu SM. Connexin35/36 gap junction proteins are expressed in photoreceptors of the tiger salamander retina. J Comp Neurol. 2004;470(1):1-12. doi: 10.1002/cne.10967. PubMed PMID: 14755521.
153. Custer NV. Structurally specialized contacts between the photoreceptors of the retina of the axolotl. J Comp Neurol. 1973;151(1):35-56. doi: 10.1002/cne.901510104. PubMed PMID: 4731301.
154. Kraft TW, Burkhardt DA. Telodendrites of cone photoreceptors: structure and probable function. J Comp Neurol. 1986;249(1):13-27. doi: 10.1002/cne.902490103. PubMed PMID: 2426311.
155. Hess M, Melzer RR, Smola U. The pattern of cone pedicles and horizontal cells in the retina of the European anchovy, Engraulis encrasicolus L. (Engraulididae, Clupeiformes). J Submicrosc Cytol Pathol. 2002;34(4):355-65. PubMed PMID: 12575834.
156. Stell WK. The structure and morphologic relations of rods and cones in the retina of the spiny dogfish, Squalus Comp Biochem Physiol. 1972;42A(1):141-51. PubMed PMID: 4402704.
157. Kolb H, West RW. Synaptic connections of the interplexiform cell in the retina of the cat. J Neurocytol. 1977;6(2):155-70. PubMed PMID: 853310.
158. Smith RG, Freed MA, Sterling P. Microcircuitry of the dark-adapted cat retina: functional architecture of the rod-cone network. J Neurosci. 1986;6(12):3505-17. PubMed PMID: 3794785.
159. Ahnelt P, Keri C, Kolb H. Identification of pedicles of putative blue-sensitive cones in the human retina. J Comp Neurol. 1990;293(1):39-53. doi: 10.1002/cne.902930104. PubMed PMID: 2312791.

160. Raviola E, Gilula NB. Intramembrane organization of specialized contacts in the outer plexiform layer of the retina. A freeze-facture study in monkeys and rabbits. . J Cell Biol. 1975;65(1):192-222. PubMed Central PMCID: PMCPMC2111162.

161. Hornstein EP, Verweij J, Li PH, Schnapf JL. Gap-junctional coupling and absolute sensitivity of photoreceptors in macaque retina. J Neurosci. 2005;25(48):11201-9. doi: 10.1523/JNEUROSCI.3416-05.2005. PubMed PMID: 16319320.

162. Tsukamoto Y, Masarachia P, Schein SJ, Sterling P. Gap junctions between the pedicles of macaque foveal cones. Vision Research. 1992;32(10):1809-15. doi: 10.1016/0042-6989(92)90042-h.

163. Westerfield M. The zebrafish book. A guide for the laboratory use of zebrafish (Danio rerio). University of Oregon Press, Eugene 2000.

164. Conrad GW, Bee JA, Roche SM, Teillet M-A. Fabrication of microscalpels by electrolysis of tungsten wire in a meniscus. Journal of Neuroscience Methods. 1993;50(1):123-7. doi: 10.1016/0165-0270(93)90062-v.

165. Ile KE, Kassen S, Cao C, Vihtehlic T, Shah SD, Mousley CJ, et al. Zebrafish class 1 phosphatidylinositol transfer proteins: PITPbeta and double cone cell outer segment integrity in retina. Traffic. 2010;11(9):1151-67. doi: 10.1111/j.1600-0854.2010.01085.x. PubMed PMID: 20545905; PubMed Central PMCID: PMCPMC2919645.

166. Alvarez-Delfin K, Morris AC, Snelson CD, Gamse JT, Gupta T, Marlow FL, et al. Tbx2b is required for ultraviolet photoreceptor cell specification during zebrafish retinal development. Proc Natl Acad Sci U S A. 2009;106(6):2023-8. doi: 10.1073/pnas.0809439106. PubMed PMID: 19179291; PubMed Central PMCID: PMCPMC2632714.

167. DuVal MG, Oel AP, Allison WT. gdf6a is required for cone photoreceptor subtype differentiation and for the actions of tbx2b in determining rod versus cone photoreceptor fate. PLoS One. 2014;9(3):e92991. doi: 10.1371/journal.pone.0092991. PubMed PMID: 24681822; PubMed Central PMCID: PMCPMC3969374.

168. Burkhardt DA, Hassin G, Levine JS, MacNichol EF. Electrical responses and photopigments of twin cones in the retina of the walleye. The Journal of Physiology. 1980;309(1):215-28. doi: 10.1113/jphysiol.1980.sp013505.

169. Ribelayga C, Cao Y, Mangel SC. The circadian clock in the retina controls rod-cone coupling. Neuron. 2008;59(5):790-801. doi: 10.1016/j.neuron.2008.07.017. PubMed PMID: 18786362.

170. Biehlmaier O, Neuhauss SC, Kohler K. Synaptic plasticity and functionality at the cone terminal of the developing zebrafish retina. J Neurobiol. 2003;56(3):222-36. doi: 10.1002/neu.10243. PubMed PMID: 12884262.
171. Schmidt QD, Allison WT. Spinules as a source of retinal synaptic plasticity following cone ablation. In Preparation.
172. Kolb H, Goede P, Roberts S, McDermott R, Gouras P. Uniqueness of the S-cone pedicle in the human retina and consequences for color processing. J Comp Neurol. 1997;386(3):443-60. PubMed PMID: 9303428.
173. Ahnelt P, Pflug R. Telodendrial contacts between foveolar cone pedicles in the human retina. Experientia. 1986;42(3):298-300. doi: 10.1007/bf01942512.
174. Rubinstein R, Thu CA, Goodman KM, Wolcott HN, Bahna F, Mannepalli S, et al. Molecular logic of neuronal self-recognition through protocadherin domain interactions. Cell. 2015;163(3):629-42. doi: 10.1016/j.cell.2015.09.026. PubMed PMID: 26478182; PubMed Central PMCID: PMCPMC4624033.
175. Leung LC, Harris WA, Holt CE, Piper M. NF-Protocadherin Regulates Retinal Ganglion Cell Axon Behaviour in the Developing Visual System. PLoS One. 2015;10(10):e0141290. doi: 10.1371/journal.pone.0141290. PubMed PMID: 26489017; PubMed Central PMCID: PMCPMC4619323.
176. Leung LC, Urbancic V, Baudet ML, Dwivedy A, Bayley TG, Lee AC, et al. Coupling of NF-protocadherin signaling to axon guidance by cue-induced translation. Nat Neurosci. 2013;16(2):166-73. doi: 10.1038/nn.3290. PubMed PMID: 23292679; PubMed Central PMCID: PMCPMC3701881.
177. Shelly M, Cancedda L, Lim BK, Popescu AT, Cheng PL, Gao H, et al. Semaphorin3A regulates neuronal polarization by suppressing axon formation and promoting dendrite growth. Neuron. 2011;71(3):433-46. doi: 10.1016/j.neuron.2011.06.041. PubMed PMID: 21835341; PubMed Central PMCID: PMCPMC3164872.
178. Marchiafava PL, Strettoi E, Alpigiani V. Intracellular recording from single and double cone cells isolated from the fish retina (Tinca tinca). Exp Biol. 1985;44(3):173-80. PubMed PMID: 3851743.
179. Marchiafava PL. Cell coupling in double cones of the fish retina. Proceedings of the Royal Society B: Biological Sciences. 1985;226(1243):211-5. doi: 10.1098/rspb.1985.0091.

180. Pignatelli V, Champ C, Marshall J, Vorobyev M. Double cones are used for colour discrimination in the reef fish, Rhinecanthus aculeatus. Biol Lett. 2010;6(4):537-9. doi: 10.1098/rsbl.2009.1010. PubMed PMID: 20129950; PubMed Central PMCID: PMCPMC2936199.
181. Ohtsuka T. Spectral sensitivities of seven morphological types of photoreceptors in the retina of the turtle, Geoclemys reevesii. J Comp Neurol. 1985;237(2):145-54. doi: 10.1002/cne.902370202. PubMed PMID: 4031119.
182. Bartsch U, Oriyakhel W, Kenna PF, Linke S, Richard G, Petrowitz B, et al. Retinal cells integrate into the outer nuclear layer and differentiate into mature photoreceptors after subretinal transplantation into adult mice. Experimental Eye Research. 2008;86(4):691-700. doi: 10.1016/j.exer.2008.01.018.
183. Gonzalez-Cordero A, West EL, Pearson RA, Duran Y, Carvalho LS, Chu CJ, et al. Photoreceptor precursors derived from three-dimensional embryonic stem cell cultures integrate and mature within adult degenerate retina. Nature Biotechnology. 2013;31(8):741-7. doi: 10.1038/nbt.2643.
184. Takechi M, Hamaoka T, Kawamura S. Fluorescence visualization of ultraviolet-sensitive cone photoreceptor development in living zebrafish. FEBS Letters. 2003;553(1-2):90-4. doi: 10.1016/s0014-5793(03)00977-3.
185. D'Orazi FD, Zhao XF, Wong RO, Yoshimatsu T. Mismatch of Synaptic Patterns between Neurons Produced in Regeneration and during Development of the Vertebrate Retina. Curr Biol. 2016;26(17):2268-79. doi: 10.1016/j.cub.2016.06.063. PubMed PMID: 27524481.
186. Hamaoka T, Takechi M, Chinen A, Nishiwaki Y, Kawamura S. Visualization of rod photoreceptor development using GFP-transgenic zebrafish. Genesis. 2002;34(3):215-20. doi: 10.1002/gene.10155. PubMed PMID: 12395387.
187. Schiavo G, Benfenati F, Poulain B, Rossetto O, Polverino de Laureto P, DasGupta BR, et al. Tetanus and botulinum-B neurotoxins block neurotransmitter release by proteolytic cleavage of synaptobrevin. Nature. 1992;359(6398):832-5. doi: 10.1038/359832a0. PubMed PMID: 1331807.
188. Terada N, Hamazaki T, Oka M, Hoki M, Mastalerz DM, Nakano Y, et al. Bone marrow cells adopt the phenotype of other cells by spontaneous cell fusion. Nature. 2002;416(6880):542-5. doi: 10.1038/nature730. PubMed PMID: 11932747.

189. Ying QL, Nichols J, Evans EP, Smith AG. Changing potency by spontaneous fusion. Nature. 2002;416(6880):545-8. doi: 10.1038/nature729. PubMed PMID: 11932748.
190. Alvarez-Dolado M, Pardal R, Garcia-Verdugo JM, Fike JR, Lee HO, Pfeffer K, et al. Fusion of bone-marrow-derived cells with Purkinje neurons, cardiomyocytes and hepatocytes. Nature. 2003;425(6961):968-73. doi: 10.1038/nature02069. PubMed PMID: 14555960.
191. Kemp K, Wilkins A, Scolding N. Cell fusion in the brain: two cells forward, one cell back. Acta Neuropathol. 2014;128(5):629-38. doi: 10.1007/s00401-014-1303-1. PubMed PMID: 24899142; PubMed Central PMCID: PMCPMC4201757.
192. Johansson CB, Youssef S, Koleckar K, Holbrook C, Doyonnas R, Corbel SY, et al. Extensive fusion of haematopoietic cells with Purkinje neurons in response to chronic inflammation. Nat Cell Biol. 2008;10(5):575-83. doi: 10.1038/ncb1720. PubMed PMID: 18425116; PubMed Central PMCID: PMCPMC4230437.
193. Weimann JM, Johansson CB, Trejo A, Blau HM. Stable reprogrammed heterokaryons form spontaneously in Purkinje neurons after bone marrow transplant. Nat Cell Biol. 2003;5(11):959-66. doi: 10.1038/ncb1053. PubMed PMID: 14562057.
194. Zhao C, Yasumura D, Li X, Matthes M, Lloyd M, Nielsen G, et al. mTOR-mediated dedifferentiation of the retinal pigment epithelium initiates photoreceptor degeneration in mice. J Clin Invest. 2011;121(1):369-83. doi: 10.1172/JCI44303. PubMed PMID: 21135502; PubMed Central PMCID: PMCPMC3007156.
195. Mesnil M, Piccoli C, Tiraby G, Willecke K, Yamasaki H. Bystander killing of cancer cells by herpes simplex virus thymidine kinase gene is mediated by connexins. Proceedings of the National Academy of Sciences of the United States of America. 1996;93(5):1831-5. doi: DOI 10.1073/pnas.93.5.1831. PubMed PMID: WOS:A1996TY96400018; PubMed Central PMCID: PMCPMC39867.
196. Bi WL, Parysek LM, Warnick R, Stambrook PJ. In vitro evidence that metabolic cooperation is responsible for the bystander effect observed with HSV tk retroviral gene therapy. Hum Gene Ther. 1993;4(6):725-31. doi: 10.1089/hum.1993.4.6-725. PubMed PMID: 8186287.
197. Pitts JD. Cancer gene therapy: A bystander effect using the gap junctional pathway. Molecular Carcinogenesis. 1994;11(3):127-30. doi: 10.1002/mc.2940110302.

198. Frantseva MV, Kokarovtseva L, Perez Velazquez JL. Ischemia-induced brain damage depends on specific gap-junctional coupling. J Cereb Blood Flow Metab. 2002;22(4):453-62. doi: 10.1097/00004647-200204000-00009. PubMed PMID: 11919516.

199. Wang Y, Denisova JV, Kang KS, Fontes JD, Zhu BT, Belousov AB. Neuronal gap junctions are required for NMDA receptor-mediated excitotoxicity: implications in ischemic stroke. J Neurophysiol. 2010;104(6):3551-6. doi: 10.1152/jn.00656.2010. PubMed PMID: 20943940; PubMed Central PMCID: PMCPMC3007655.

200. Das S, Lin D, Jena S, Shi A, Battina S, Hua DH, et al. Protection of retinal cells from ischemia by a novel gap junction inhibitor. Biochem Biophys Res Commun. 2008;373(4):504-8. doi: 10.1016/j.bbrc.2008.06.069. PubMed PMID: 18590704; PubMed Central PMCID: PMCPMC2529171.

201. Young RW. Cell death during differentiation of the retina in the mouse. J Comp Neurol. 1984;229(3):362-73. doi: 10.1002/cne.902290307. PubMed PMID: 6501608.

202. Georges P, Madigan MC, Provis JM. Apoptosis during development of the human retina: Relationship to foveal development and retinal synaptogenesis. The Journal of Comparative Neurology. 1999;413(2):198-208. doi: 10.1002/(sici)1096-9861(19991018)413:2<198::aid-cne2>3.0.co;2-j.

203. Perry VH, Henderson Z, Linden R. Postnatal changes in retinal ganglion cell and optic axon populations in the pigmented rat. J Comp Neurol. 1983;219(3):356-68. doi: 10.1002/cne.902190309. PubMed PMID: 6619343.

204. Cusato K, Bosco A, Rozental R, Guimaraes CA, Reese BE, Linden R, et al. Gap junctions mediate bystander cell death in developing retina. J Neurosci. 2003;23(16):6413-22. PubMed PMID: 12878681.

205. Kranz K, Paquet-Durand F, Weiler R, Janssen-Bienhold U, Dedek K. Testing for a gap junction-mediated bystander effect in retinitis pigmentosa: secondary cone death is not altered by deletion of connexin36 from cones. PLoS One. 2013;8(2):e57163. doi: 10.1371/journal.pone.0057163. PubMed PMID: 23468924; PubMed Central PMCID: PMCPMC3584123.

206. Striedinger K, Petrasch-Parwez E, Zoidl G, Napirei M, Meier C, Eysel UT, et al. Loss of connexin36 increases retinal cell vulnerability to secondary cell loss. Eur J Neurosci. 2005;22(3):605-16. doi: 10.1111/j.1460-9568.2005.04228.x. PubMed PMID: 16101742.

207. Paschon V, Higa GS, Resende RR, Britto LR, Kihara AH. Blocking of connexin-mediated communication promotes neuroprotection during acute degeneration induced by mechanical trauma. PLoS One. 2012;7(9):e45449. doi: 10.1371/journal.pone.0045449. PubMed PMID: 23029016; PubMed Central PMCID: PMCPMC3447938.

208. Pennesi ME, Michaels KV, Magee SS, Maricle A, Davin SP, Garg AK, et al. Long-term characterization of retinal degeneration in rd1 and rd10 mice using spectral domain optical coherence tomography. Invest Ophthalmol Vis Sci. 2012;53(8):4644-56. doi: 10.1167/iovs.12-9611. PubMed PMID: 22562504; PubMed Central PMCID: PMCPMC3394742.

209. Gargini C, Terzibasi E, Mazzoni F, Strettoi E. Retinal organization in the retinal degeneration 10 (rd10) mutant mouse: a morphological and ERG study. J Comp Neurol. 2007;500(2):222-38. doi: 10.1002/cne.21144. PubMed PMID: 17111372; PubMed Central PMCID: PMCPMC2590657.

210. Humphries MM, Rancourt D, Farrar GJ, Kenna P, Hazel M, Bush RA, et al. Retinopathy induced in mice by targeted disruption of the rhodopsin gene. Nat Genet. 1997;15(2):216-9. doi: 10.1038/ng0297-216. PubMed PMID: 9020854.

211. Cepko CL, Vandenberghe LH. Retinal gene therapy coming of age. Hum Gene Ther. 2013;24(3):242-4. doi: 10.1089/hum.2013.050. PubMed PMID: 23458444; PubMed Central PMCID: PMCPMC4530353.

212. Marc RE, Jones BW, Watt CB, Strettoi E. Neural remodeling in retinal degeneration. Progress in Retinal and Eye Research. 2003;22(5):607-55. doi: 10.1016/s1350-9462(03)00039-9.

213. Jones BW, Kondo M, Terasaki H, Lin Y, McCall M, Marc RE. Retinal remodeling. Jpn J Ophthalmol. 2012;56(4):289-306. doi: 10.1007/s10384-012-0147-2. PubMed PMID: 22644448; PubMed Central PMCID: PMCPMC3726038.

214. Peng YW, Hao Y, Petters RM, Wong F. Ectopic synaptogenesis in the mammalian retina caused by rod photoreceptor-specific mutations. Nat Neurosci. 2000;3(11):1121-7. doi: 10.1038/80639. PubMed PMID: 11036269.

215. Jones BW, Watt CB, Frederick JM, Baehr W, Chen CK, Levine EM, et al. Retinal remodeling triggered by photoreceptor degenerations. J Comp Neurol. 2003;464(1):1-16. doi: 10.1002/cne.10703. PubMed PMID: 12866125.

216. Jones BW, Kondo M, Terasaki H, Watt CB, Rapp K, Anderson J, et al. Retinal remodeling in the Tg P347L rabbit, a large-eye model of retinal degeneration. J Comp

Neurol. 2011;519(14):2713-33. doi: 10.1002/cne.22703. PubMed PMID: 21681749; PubMed Central PMCID: PMCPMC3894993.